

**USING FLOW THROUGH REACTORS TO STUDY THE NON-  
REDUCTIVE BIOMINERALIZATION OF URANIUM PHOSPHATE  
MINERALS UNDER ANAEROBIC CONDITIONS**

A Thesis  
Presented to  
The Academic Faculty

by

Anna Rachel Williams

In Partial Fulfillment  
of the Requirements for the Degree  
Master of Science in the  
School of Earth and Atmospheric Sciences

Georgia Institute of Technology  
May, 2012

**USING FLOW THROUGH REACTORS TO STUDY THE NON-  
REDUCTIVE BIOMINERALIZATION OF URANIUM PHOSPHATE  
MINERALS UNDER ANAEROBIC CONDITIONS**

Approved by:

Dr. Martial Taillefert, Advisor  
School of Earth and Atmospheric Sciences  
*Georgia Institute of Technology*

Dr. Thomas DiChristina  
School of Biology  
*Georgia Institute of Technology*

Dr. Philippe Van Cappellen  
School of Earth and Environmental Sciences  
*University of Waterloo*

Date Approved: April 2, 2012

## ACKNOWLEDGEMENTS

It takes a village to raise a geochemist. I am extremely grateful for all the people in my life who helped me complete this project. The enthusiasm and patience of my advisor, Dr. Martial Taillefert was the driving force behind the completion of this project. I am deeply grateful for his constant faith in me when I would automatically assume that I had failed. I would also like to thank my committee members Dr. Philippe Van Cappellen and Dr. Tom DiChristina for their input. I also appreciate Tom's sympathy from when I fainted in his and Martial's class because I was afraid of messing up my nitrogen cycle presentation.

There are so many people who helped me emotionally during this time. Thank you so much to everyone who fed me, made me laugh, or held me as I cried. These people include my former and current classmates and best friends forever: Kate Salome, Lin Hui, Jordan Beckler, Colin Dean, Keaton Belli, Morris Jones, Emily Saad, and Beth Tomaszewski, Jake Leech, Jessica Moerman, Stacy Carolin, Laura King, and Michelle Oakes, Nadia Szeinbaum, Alica Nobles, and Seng Kew Wee. I also want to thank my housemate/bff Ann Curley for taking me in and sharing her wine with me and giving me pep-talks, and Stephanie Briggs for all the meals, adventures, and bruises. I am fortunate to have been a part of a community of people this intelligent, funny, and kind.

Finally I would like to thank my parents whose guidance strongly influenced my decision to return to graduate school. I also benefitted from the close proximity of my loving grandparents Gran Ann and Nandy and my brother Tom who would always boost my spirits.

## TABLE OF CONTENTS

	Page
ACKNOWLEDGEMENTS	iii
LIST OF TABLES	v
LIST OF FIGURES	vi
 <u>CHAPTER</u>	
1 CHAPTER 1 INTRODUCTION	1
2 CHAPTER 2 METHODS	11
2.1 Modification of Tessier’s Sequential Extraction Method	11
2.2 Flow Through Reactors	13
2.3 Analytical Methods	18
2.4 Thermodynamic Calculations	24
2.5 One-dimensional Transient Reactive Transport Model	25
3 CHAPTER 3 RESULTS	27
3.1 Results from the Modification of a Sequential Extraction Scheme	28
3.2 Composition of the Effluent from Flow Through Reactor Incubations	31
4 CHAPTER 4 DISCUSSION	41
4.1 Modified Sequential Extraction Scheme	43
4.2 Transport Parameters Calculated from Inert Tracer	45
4.3 Respiration Processes in Anaerobic ORFRC Soils	47
4.3 Evidence for Biomineralization of Uranium Phosphate Minerals	52
4.4 Implications and Future Research	54
5 CHAPTER 5 CONCLUSIONS	56
APPENDIX A: Rate Calculations Fitted to Data	58
REFERENCES	62

## LIST OF TABLES

	Page
Table 1. Composition of the simulated groundwater used in this study that reflects the geochemical conditions of Area 3 at the Oak Ridge Field Research Center, Oak Ridge (TN) (Beazley et al., 2011). All chemicals were reagent grade and prepared in MilliQ water (Barnstead).	15
Table 2. Average transport parameters calculated by a one-dimensional advection dispersion model of the average bromide concentrations in flow through reactor effluent.	46
Table 3. Net reaction rates for dissolved species in the flow through reactors (pH 5.5) determined by the one-dimensional reactive transport model.	51

## LIST OF FIGURES

	Page
Figure 1: Speciation of 200 $\mu\text{M}$ $\text{UO}_2^{2+}$ , 200 $\mu\text{M}$ $\text{PO}_4^{3-}$ , and 200 $\mu\text{M}$ $\text{Ca}^{2+}$ as a function of pH at $\text{PCO}_2 = 10^{-3.5}$ and as predicted using the equilibrium modeling program MINEQL (Schecher and McAvoy, 2001). Taken from (Beazley 2009).	4
Figure 2: Schematic of the Flow Through Reactor set-up. Four reactors were used during this experiment. Blue arrows indicate simulated groundwater flow path. Reactors were incubated in an anaerobic chamber for the anoxic phase of the experiment.	15
Figure 3: Timeline of the Flow Through Reactor study showing the oxidation state and different amendments made to the reactors. The long-term G2P amended reactors were run in triplicate.	17
Figure 4: ICP-MS detector counts of internal standard and quality control samples (SLRS-5 and calibration blank) over the duration of a typical analysis for total dissolved uranium. SLRS-5 Certified material and quality control standards confirm that the analysis is accurate when the internal standard correction for instrument drift is applied to each sample.	20
Figure 5: Ion chromatogram acquired in the presence of 1 mM $\text{Cl}^-$ , $\text{NO}_2^-$ , $\text{Br}^-$ , $\text{NO}_3^-$ , G2P, $\text{PO}_4^{3-}$ and $\text{SO}_4^{2-}$ .	21
Figure 6. Typical examples of voltammograms obtained in-line in a flow through reactor to determine the concentration of (a) dissolved $\text{O}_2$ by linear sweep voltammetry and (b) dissolved $\text{Fe}^{2+}$ , $\text{Mn}^{2+}$ , and $\Sigma\text{H}_2\text{S}$ by square wave voltammetry. The later species were never detected during these flow through incubations. The MES creates a peak at ca. -1.6 V that interferes with the $\text{Mn}^{2+}$ measurement.	23
Figure 7 (A) Uranium adsorbed to lepidocrocite and (B) lab-synthesized uranyl phosphate precipitate extracted by the traditional Tessier method compared to a modification of the first step. Only the first step of the Tessier method was modified by adding either 10 mM NTA or Na-citrate. The pH of the first step was lowered from 7 to 4.5. Standard deviation represents variation on duplicate samples.	29
Figure 8. Solid phase mixture of uranium adsorbed to lepidocrocite and lab-synthesized uranyl phosphate precipitate extracted by the original Tessier method compared to a modification of the first step. The first bar represents the true percentage of uranium of the mineral/adsorbed iron oxide mixture. Standard deviation represents variation on duplicate samples.	29

Figure 9. Effluent concentrations of bromide measured (symbols) and calculated from the transient 1D transport model (line) in the four FTRs over time during the incubation: a) short-term G2P amended reactor (triangles); and b) through c) the three long-term G2P amended reactors (circles). Bromide was added at days 0, 101, and 164 (101 and 164 indicated by vertical dashed lines). Error bars represent analytical error on the measurement in each reactor. **32**

Figure 10. Average concentrations of oxygen, nitrate, nitrite, and sulfate in the three long term (black symbols) and the one short-term (open symbols) G2P amended reactors. Nitrite concentrations are represented by triangles. Error bars on solid symbols refer to the standard deviation of triplicate reactors. Error bars on open symbols refer to analytical error. **34**

Figure 11. pH and concentration of G2P, total soluble phosphate, and uranium measured in the effluent of the 3 long-term G2P amended FTRs (closed symbols) and 1 short-term G2P amended FTR (open symbols). Blue symbols correspond to G2P measurements. Error bars on solid symbols refer to the standard deviation of triplicate reactors. Error bars on open symbols refer to analytical error. **36**

Figure 12. Uranium adsorption curve from batch experiments and a thermodynamic model that describes the adsorption process assuming iron oxides as the main adsorbent. Batch data represent single measurements; error bars of measurements are within symbol. **38**

Figure 13. Total uranium recovered from Tessier's sequential extraction scheme performed on soils from the short (FTR 2) and long term G2P amended (FTR 1,3,4) reactors after incubation with G2P and 200  $\mu\text{M}$  uranyl acetate. Error bars represent the results of triplicate samples. Note larger scale on FTR 2 graph. **40**

## SUMMARY

Uranium contaminations of the subsurface in the vicinity of nuclear materials processing sites pose a health risk as the uranyl ion in its oxidized state, U(VI), is highly mobile in aquifers. Current remediation strategies such as pump and treat or excavation are invasive and expensive to implement on a large scale. In situ bioremediation represents an alternative strategy that uses the ability of local microbial communities to immobilize contaminants and is actively studied for uranium remediation. The immobilization of U(VI) in groundwater is achieved either by bioreduction to solid uraninite (U(IV)), adsorption to the soil matrix, or non-reductive precipitation of uranium phosphate minerals through the activity of bacterial phosphatases. Bioreduction has been widely studied for remediation of the saturated zone, as anaerobic conditions typically prevail in these environments. This process is only efficient at circumneutral pH, however, and the end product uraninite is unstable under aerobic conditions or in the presence of manganese oxides, nitrite, or even freshly formed iron oxides. Although non-reductive biomineralization of uranium catalyzed by bacterial phosphatase activity successfully removes uranium from the vadose zone, further studies are needed to assess the ability of microbial communities to hydrolyze organophosphate compounds in the saturated zone where oxygen is often depleted and uranium bioreduction may be significant. To investigate this process under anaerobic conditions, low pH soil samples from a uranium contaminated site at the Oak Ridge Field Research Center were incubated anaerobically in flow through reactors in the presence of exogenic organophosphate compounds to stimulate the natural microbial communities in the original soil matrix.



Aqueous uranium was injected continuously in the reactors to determine the fraction of uranium removed during these incubations. The reactors amended with organophosphate produced inorganic phosphate in the effluent, suggesting that bacterial phosphatase activity can be stimulated even in anaerobic environments at low pH. Removal of U(VI) in a control amended with organophosphate over a short time period was similar compared to reactors amended with organophosphate for long times suggesting that adsorption may also play a role in U(VI) immobilization. A sequential extraction technique was optimized to differentiate the fraction of uranium loosely adsorbed and the fraction of uranium precipitated as phosphate minerals and batch adsorption experiments were performed to obtain thermodynamic parameters that could be used to predict the fraction of U(VI) adsorbed onto the soil matrix. Results indicated that 100% uranium adsorption was favorable from pH 5 to 10 (without the presence of phosphate). Extraction of sediments, however, indicated that most of the solid phase uranium was incorporated as uranium phosphate mineral in both long and short-term amended reactors. Overall, these results demonstrate that the biomineralization of uranium phosphate minerals is a viable bioremediation strategy in both the vadose and saturated zones of aquifers at both low and high pH, provided an organophosphate source is available.

# **CHAPTER 1**

## **INTRODUCTION**

Since World War Two, the research and development of nuclear materials and weapons has lead to the contamination of soils and groundwater at many sites across the United States. The National Defense Authorization Act of 1995 directed the Department of Energy to assesss and describe waste generated during each step of nuclear materials production and the extent of radioactive materials that currently exist, including contaminated environmental media (DOE 1997). The results showed that total weapons production had contributed to 1800 million cubic meters of contaminated groundwater and 79 million cubic meters of soil (DOE 1997). Three of these sites (Oak Ridge, TN, Hanford, WA, and Rifle, CO) were designated as DOE Integrated Field Research Sites with the objective of conducting research to remediate uranium and other contaminants associated with munitions processing.

The Oak Ridge Y-12 plant was built in 1943 under the Manhattan Project, and produced highly enriched uranium that is used for nuclear materials processing and for the production of nuclear weapons. The waste from the chemical separation process used to enrich uranium was disposed of in the S-3 ponds in Area 3 of ORFRC. From 1950 to 1983,  $3.2 \times 10^8$  liters of waste containing nitric acid and uranium was disposed of in the ponds. As the S-3 ponds contained no physical or chemical barrier from the surrounding subsurface, the wastewater was able to infiltrate the surrounding groundwater, leading to a contamination plume that extends 4 km down gradient from the ponds (DOE 1997). In 1988, the ponds were denitrified and capped with asphalt in an attempt to limit further

contamination (Brooks 2001). Other contaminants associated with the waste from the S-3 ponds include technetium-99, nitrate, thorium, and volatile organic compounds. Groundwater levels of uranium can be as high as 250  $\mu\text{M}$ , and nitrate levels as high as 60 mM (Jardine et al. 2006). The Environmental Protection Agency defines the maximum contaminant level (MCL) for tap water levels of uranium to be 126 nM.

The large-scale contamination at ORFRC presents a challenge for current remediation strategies. *Ex situ* techniques such as pump and treat and excavation and treatment physically remove the contaminated soil or groundwater from a site for treatment and storage or return the treated media back to the original site. These procedures are invasive and therefore difficult to implement on a large scale. Additionally, the removed contaminants must be stored, increasing the risk of exposure (Gavrilescu et al. 2009). Alternatively, contaminants can be treated or immobilized with *in situ* methods such as permeable reactive barriers, natural attenuation, or bioremediation (Gavrilescu et al. 2009). These methods involve treating or immobilizing a contaminant within a site, and are generally less invasive and more economical for large-scale remediation sites such as the ORFRC.

Permeable reactive barriers consist of a wall of reactive material extending below the water table that is placed down gradient from a contamination plume (US EPA). The barrier intercepts the plume and removes contaminants from the groundwater chemically by adsorption, reduction, or ion exchange or biologically through microbial activity (Gavrilescu et al. 2009). Over time, the used reactive material within the barrier must be maintained and/or replaced, and properly disposed of or stored. PRBs are most efficient and cost effective for narrow contamination plumes and near surface contamination

(Gavrilescu et al. 2009), and the magnitude of contamination at the ORFRC could present a physical and economic challenge to the installation and maintenance of PRBs.

Natural attenuation is a more economical alternative approach for large contamination sites. This technique allows the natural processes at a specific site to contain and reduce the concentration of pollutants without human intervention (US EPA). Environmental factors such as pH, redox conditions, and the presence of other chemical species must be taken into consideration, as uranium speciation is strongly dependent on the chemistry of the site. Under specific conditions uranium immobilization occurs naturally over time by adsorption or by incorporation into minerals (Langmuir, 1997; Gavrilescu et al. 2009).

In aerobic environments, uranium exists in the soluble U(VI) oxidation state as the uranyl ion, while anaerobic conditions promote the stability of insoluble U(IV) species (Langmuir 1997). Interactions with other aqueous species and pH determine the mobility of the uranyl ion. At low pH, the uranyl ion is positively charged and exists as either  $\text{UO}_2^{2+}$ ,  $\text{UO}_2\text{OH}^+$ , or U(VI) phosphate complexes if phosphate is present (Sandino et al. 1992), and its mobility can be limited by adsorption onto soils enriched in iron or manganese oxides (Langmuir 1997). From pH 4 to 6, uranyl ions can adsorb directly to the soil (Barnett et al. 2002), or compete with phosphate for adsorption sites. The presence of phosphate can even lower the pH of the adsorption edge from 4 to 2 by formation of ternary U(VI) phosphate surface complexes on iron oxides (Cheng et al. 2004). Similarly, negatively charged NOM can increase adsorption of U(VI) at low pH (Lenhart et al. 1999). At pH values above 7, the presence of carbonate stabilizes U(VI) as aqueous complexes such as  $\text{UO}_2(\text{CO}_3)_2^{2-}$  and  $\text{UO}_2(\text{CO}_3)_3^{4-}$  (Langmuir 1997). These

complexes and ternary uranyl-calcium-carbonato complexes ( $\text{Ca}_2\text{UO}_2(\text{CO}_3)_3$  and  $\text{CaUO}_2(\text{CO}_3)_3^{2-}$ ) even promote the desorption of U(VI) (Stewart et al. 2010) and the dissolution of uranium bearing minerals (Zhou et al. 2005) (Figure 1).

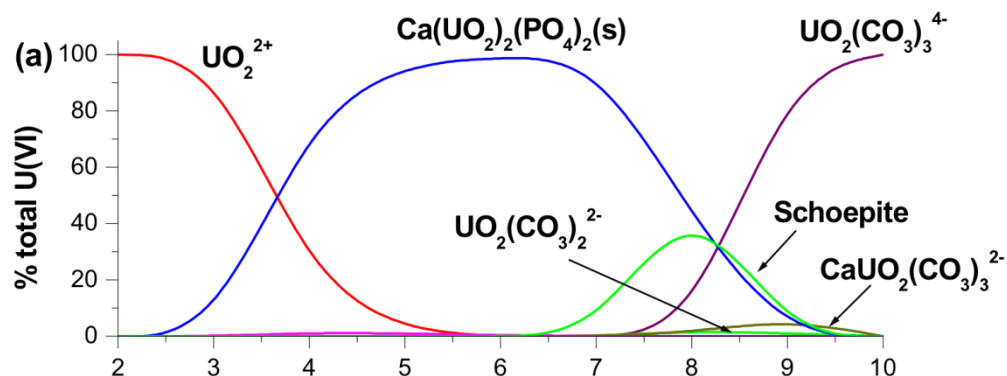


Figure 1. Speciation of 200 μM  $\text{UO}_2^{2+}$ , 200 μM  $\text{PO}_4^{3-}$ , and 200 μM  $\text{Ca}^{2+}$  as a function of pH at  $\text{PCO}_2 = 10^{-3.5}$  and as predicted using the equilibrium modeling program MINEQL (Schecher and McAvoy, 2001). Adapted from (Beazley, 2009).

Uranium minerals exist in both aerobic (as U(VI)) and anaerobic (as U(IV)) conditions. Autunite/meta-autunite minerals [ $\text{X}^{2+}(\text{UO}_2)_2(\text{PO}_4)_2$ ] can be stable over long periods of time at acidic to neutral pH range (Fuller et al. 2003) (Figure 1). One study postulates that Ba-meta-autunite samples at a site in Australia have been stable for 50,000 years, assuming a constant weathering rate (Jerden et al. 2003). Simulated weathering experiments conducted on U(VI) incorporated into hydroxyapatite [ $\text{Ca}_5(\text{PO}_4)_3(\text{OH})$ ] also showed resistance to dissolution (Shelobolina et al. 2009). The U(IV) mineral uraninite ( $\text{UO}_2$ ) is sparingly soluble at circumneutral pH under anoxic conditions, though monomeric U(IV) compounds have recently been identified as a product of chemical or biological reduction (Fletcher et al. 2010; Boyanov et al. 2011). Aqueous U(VI) can be

chemically reduced to uraninite by Fe(II) adsorbed to iron oxides (Liger et al. 1999; Boland et al. 2011) or adsorbed sulfides (Wersin et al. 1994). Depending on site conditions, uranium minerals could form naturally at different rates, rendering natural attenuation inefficient for larger areas of contamination.

Bioremediation represents an alternative *in situ* strategy that promotes the formation of solid phase uranium by stimulating local microbial communities. *In situ* bioremediation may immobilize contaminants through either bioreduction of aqueous U(VI) to solid uraninite (U(IV)) or non-reductive precipitation of uranium phosphate minerals (Lovley et al. 1991; Macaskie et al. 1994; Beazley et al. 2007). Bioreduction has been widely studied for remediation of the saturated zone, as anaerobic conditions typically prevail in these environments. A variety of metal resistant bacteria have been isolated that are able to enzymatically reduce U(VI) to U(IV), including some species that even have the ability to grow on U(VI) in the absence of a more favorable terminal electron acceptor (Tebo et al. 1998; Wade et al. 2000). Notably, dissimilatory metal and sulfate reducing bacteria such as *Shewanella putrefaciens*, *Geobacter sulfurreducens*, *Desulfovibrio desulfuricans*, and more recently *Anaeromyxobacter dehalogenans* have demonstrated the ability to reduce U(VI) to U(IV) either enzymatically or by indirect abiotic reduction from ferrous iron (Lovley et al. 1992; Fredrickson et al. 2000; Behrends et al. 2005; Sanford et al. 2007). Bioreduction is only efficient at circumneutral pH, however, and the end product uraninite is unstable under aerobic conditions or in the presence of manganese and iron oxides, nitrate, or, nitrite (Senko et al. 2002; Wan et al. 2005). The high levels of nitrate and low pH at the ORFRC site have made this remediation strategy difficult to implement in the past. The treatment zone first had to be

conditioned to remove nitrate and to raise the pH (Wu et al. 2006), and further studies indicated that nitrate additions oxidized and remobilized reduced uranium (Wu et al. 2010).

The non-reductive precipitation of uranium phosphate minerals through the activity of bacterial phosphatases is currently studied as an alternative method to bioreduction. A variety of bacteria isolated from uranium contaminated sediments contain nonspecific acid phosphohydrolases or phosphatases (NSAPs) (Macaskie et al. 1994; Martinez et al. 2008; Shelobolina et al. 2009). NSAPs function most efficiently at acidic pH and have the ability to hydrolyze organic phosphate compounds, which in turn release orthophosphate that is available for cell function and the precipitation of uranium phosphate minerals (Rossolini et al. 1998). Glycerol 3-phosphate (G3P), Glycerol 2-phosphate (G2P), and tributyl phosphate have all been studied as organic phosphorus sources for the non-reductive precipitation of uranium phosphate minerals (Macaskie et al. 1994; Thomas et al. 1996; Beazley et al. 2007; Martinez et al. 2008; Beazley et al. 2011).

Numerous studies have shown that non-reductive biomineralization of uranium phosphate minerals occurs under aerobic conditions. Pure culture studies with *Citrobacter*, *Pseudomonas aeruginosa*, *Rahnella*, and *Aeromonas hydrophila* isolated from contaminated environments all displayed the ability to produce uranium phosphate minerals under aerobic conditions when provided with an organophosphate source (Macaskie et al. 1994; Thomas et al. 1996; Barnett et al. 2002; Renninger et al. 2004; Beazley et al. 2007). Other microbes such as the yeast *Saccharomyces cerevisiae* and the fungus *S. himantioides* and *B. caledonica* are also able to precipitate uranium phosphate

minerals (Ohnuki et al, 2005). The uranium phosphate precipitate has been identified as a polycrystalline  $\text{H}_2\text{UO}_2\text{PO}_4$  that is indistinguishable from uranyl phosphate precipitates formed by chemical methods (Macaskie et al. 1994). In the cases of the bacteria *Rahnella* and the fungus *S. himantoides* and *B. caledonica*, the precipitates identified by XAS included autunite or meta-autunite group minerals (Beazley et al. 2007; Fomina et al. 2007) while the precipitates formed by *Aeromonas hydrophila* in the presence of calcium at circumneutral pH were determined to consist of hydroxyapatite minerals (Shelobolina et al. 2009). In addition to pure culture studies, incubations using soils from the ORFRC have demonstrated the ability to precipitate uranium phosphate minerals in aerobic conditions when provided with an organophosphate source (Shelobolina et al. 2009; Beazley et al. 2011).

Nitrate-reducing bacteria have been widely studied in an effort to make uranium reduction more favorable by removing high nitrate levels associated with uranium contamination at the ORFRC (Akob et al. 2007; Spain et al. 2011). Denitrification, is the conversion of nitrate ( $\text{NO}_3^-$ ) to nitrogen gas ( $\text{N}_2$ ) through the intermediates nitrite ( $\text{NO}_2^-$ ) nitric oxide (NO) and nitrous oxide ( $\text{N}_2\text{O}$ ) (Vitousek et al. 1991). Denitrification is the most thermodynamically favorable respiration process after aerobic respiration (Morel et al. 1993) thus making it a strong competitor against uranium reduction, especially with the high levels of nitrate present at the ORFRC. Denitrification can be performed by individual prokaryotes or by a consortium of microbes within the soil matrix as each intermediate step requires a different enzyme (Lam et al. 2011). Dissimilatory nitrate reduction to ammonium (DNRA) is an alternative respiration pathway for nitrate that forms nitrite as intermediate. In addition to complete denitrification and DNRA, nitrate



reduction to nitrite can occur as a sole respiration process (Zumft 1997; Gonzalez et al. 2006). Nitrate respiration could be involved in the biomineralization of uranium under anaerobic, high nitrate conditions. Indeed, nitrate-reducing microorganisms have been identified in ORFRC soils. Pure culture incubations with the facultative anaerobe *Rahnella* sp isolated from ORFRC soils precipitated U(VI) phosphate minerals when fed G3P and simultaneously reduced nitrate to nitrite without production of ammonium nor dinitrogen gas (Beazley et al. 2009). Separate sediment incubations in anaerobic conditions revealed that *Rahnella* forms uranium phosphate or organophosphate precipitates even without the addition of an organophosphate source possibly by using internal organophosphate sources (Geissler et al. 2009). Uranyl phosphate precipitates were also produced simultaneously with nitrate reduction in ORFRC sediments under low pH and high nitrate conditions upon ethanol addition as electron donors, and the dominant microbe *Burkholderia fungorum* was isolated from these incubations (Michalsen et al. 2009).

As biomineralization of uranium phosphate minerals may occur under both aerobic and anaerobic conditions, the possibility exists for multiple modes of uranium immobilization under reducing conditions. Increasing numbers of studies are finding reduced U(IV) phosphate species as a product of bioreduction (Khijniak et al. 2005; Bernier-Latmani et al. 2010; Fletcher et al. 2010; Boyanov et al. 2011). In separate anaerobic pure culture studies, the bacterium *Thermoterrabacterium ferrireducens* (Khijniak et al. 2005) and *Desulfotomaculum reducens* (Bernier-Latmani et al. 2010) produced a reduced uranium phosphate species that was determined to be ningyoite [U<sub>2</sub>O(PO<sub>4</sub>)<sub>2</sub>]. Another uranium reduction study showed that the presence of phosphate

enhances uranium removal from solution by the formation of U(IV) phosphate precipitates (Boyanov et al. 2011). Phosphate does not need to be initially present in solution, however, for uranium biomineralization to occur. A study using strain UFO1 isolated from ORFRC sediments apparently utilizes internal reserves of phosphate to simultaneously precipitate both U(VI) phosphate minerals and a monomeric U(IV) species that is not uraninite (Boyanov et al. 2011). Finally, a strain of *Cellulomonas* also showed the ability to produce U(VI) phosphate minerals under reducing conditions (Sivaswamy et al. 2011).

As reducing conditions create the potential for uranium removal by reduction or precipitation of uranium phosphate minerals in addition to adsorption, determining the speciation of uranium in the solid phase is complex especially in the case of whole sediment incubations. The efficacy of any remediation treatment depends on the ability to confirm that aqueous uranium is transformed to an identifiable and stable solid phase. Past bioremediation studies have used a combination of x-ray adsorption spectroscopy (XAS), x-ray diffraction (XRD), and other fluorescence techniques as well as wet chemical techniques, such as sequential extraction methods, to analyze the speciation of uranium in the solid phase (Gavrilescu et al. 2009). Attempts have been made to apply sequential extraction techniques to radionuclide fractionation (Schultz et al. 1998; Blanco et al. 2004; Smith et al. 2009). These methods are logistically simpler than XAS, as they do not require a synchrotron and provide useful supplemental information on solid phase uranium.

The unique geochemical conditions of a site must be considered when developing a remediation strategy. This study focuses on assessing the potential for

non-reductive biomineralization of uranium as a possible remediation strategy for the Oak Ridge Field Research Center (ORFRC) in Oak Ridge, Tennessee. To investigate this process under anaerobic conditions, soil samples from a uranium contaminated site at the Oak Ridge Field Research Center were incubated anaerobically in flow through reactors in the presence of organophosphate compounds to stimulate the natural microbial communities in the original soil matrix. Aqueous uranium was injected continuously in the reactors to determine the fraction of uranium removed during these incubations. A sequential extraction technique was optimized to differentiate the fraction of uranium that was adsorbed vs. the fraction precipitated as uranium phosphate minerals. Simultaneously, adsorption experiments were performed to obtain thermodynamic parameters that could be used to predict the fraction of U(VI) adsorbed onto the soil matrix. Ultimately, this study hypothesizes that non reductive biomineralization of uranium phosphate minerals is a viable remediation strategy in anaerobic environments at the ORFRC by assessing the main anaerobic microbial respiration process taking place in these sediments, determining whether phosphate metabolism is significant in reducing conditions, and quantifying the fate of immobilized uranium.

## CHAPTER 2

### METHODS

#### 2.1 Modification of Tessier's Sequential Extraction Method

Tessier's method for the sequential extraction of metals from sediments is often used to determine the speciation of trace metals in the solid phase (Tessier et al. 1979). The original method applies 5 different leaching solutions to a 1 g soil sample sequentially as follows: 8 mL 1 M  $\text{MgCl}_2$  pH 7 for 1 hour to extract the loosely exchangeable phase, 8 mL 1 M NaOAc adjusted to pH 5 with HOAc for 6 hours to obtain the fraction bound to carbonates, 20 mL 0.04 M  $\text{NH}_2\text{OH}\cdot\text{HCl}$  in 25 % v/v HOAc at 95°C for 6 hours to extract the phase bound to Fe/Mn oxides. The fourth step targets the fraction bound to organic matter by adding 3 ml 0.02 M  $\text{HNO}_3$  and 5 ml 30%  $\text{H}_2\text{O}_2$  (pH 2) and equilibrating for 3 hours at 85°C. An additional 3 mL of 20%  $\text{H}_2\text{O}_2$  (pH 2) is added and allowed to equilibrate 3 more hours at 85°C. The sample is then cooled and 5 mL 3.2 M  $\text{NH}_4\text{OAc}$  in 20%  $\text{HNO}_3$  is added and diluted to 20 mL. Finally, the remaining material is digested in 10 mL concentrated  $\text{HNO}_3$  at 90°C (Schultz et al. 1998).

One of the goals of this study was to determine if Tessier's method could be adapted to distinguish between the fraction of adsorbed uranium and uranium phosphate mineral in a sediment sample. This extraction method was performed on uranium adsorbed to a synthesized iron oxide mineral (lepidocrocite) and uranyl phosphate precipitates containing known amounts of uranium, in order to assess the ability of the operationally defined steps to distinguish between total adsorbed uranium and a uranyl phosphate precipitate. Adjustments were made to the first step of Tessier's method to determine a leachate that would target the loosely adsorbed uranium but not dissolve the uranium phosphate mineral.

### 2.1.1 Batch Experiments

Triplicate sets of solid phase media were made that included uranium adsorbed to lepidocrocite, uranyl phosphate precipitates, and a combination of uranium adsorbed to lepidocrocite and uranyl phosphate precipitates. All reagents used were trace metal grade unless otherwise indicated. Lepidocrocite was synthesized according to the method of Schwertman and Cornell (2000). The uranium adsorbed to lepidocrocite was prepared by adding an aliquot of 200  $\mu\text{M}$  uranyl acetate to 1 g/L lepidocrocite in simulated groundwater solution (Table 1) buffered at pH 5.5 with 10 mM MES (2-morpholinoethanesulfonic acid). The uranyl phosphate precipitate was prepared chemically by combining 0.5 mM uranyl acetate and 0.5 mM phosphate ( $\text{Na}_2\text{HPO}_4$ ) in simulated groundwater buffered at pH 5.5 with MES with an equilibration time of 48 hours. After equilibration, each uranyl phosphate mixture was centrifuged, and the precipitate rinsed in MilliQ water to remove excess phosphate. Finally an aliquot of 200  $\mu\text{M}$  uranyl acetate (final concentration) was added to 10 mg/L uranyl phosphate precipitate and 1 g/L of lepidocrocite in simulated groundwater solution. All slurries were buffered at pH 5.5 with MES and allowed to equilibrate for 48 hours. The supernatants and rinse waters (from the uranyl phosphate mineral) were filtered (0.25  $\mu\text{m}$ , nitrocellulose membrane, Millipore) and analyzed for uranium by ICP-MS for mass balance calculations. Identical sets of these solid media samples were prepared at pH 7 by adjusting the pH with NaOH.

The first two steps of Tessier's original sequential extraction scheme were applied initially to samples prepared at pH 5.5, then to the samples prepared at pH 7, to provide a basic understanding of the pH control on the solid phase speciation of uranium. Percentage of uranium recovered was determined by the total amount recovered during a particular step divided by the amount of uranium used in preparing the sample. An HCL digestion was used as the final step to ensure complete recovery of uranium. Further experiments were performed with the samples prepared at pH 5.5 to enhance the recovery

of adsorbed uranium. The first extraction step of Tessier's method was altered by lowering the pH of the 1 M  $\text{MgCl}_2$  solution from 7 to 4.5 and adding 10 mM of either nitrilotriacetic acid (NTA) or sodium citrate to prevent uranium to readsorb to the solid phase.

## **2.2 Flow Through Reactors**

### **2.2.1 Experimental Design**

Flow through reactors (FTRs) were used to simulate changing groundwater conditions in 12 cm cores of soil collected from Area 3 at the Oak Ridge Field Research Center (ORFRC) in Oak Ridge, TN (Core # FWB120-06-48). The four reactors used in this experiment were 12 cm in length with a diameter of 3.8 cm (Figure 2). Simulated groundwater solution (Table 1) was pumped into the base of the FTR at a rate of 1 mL/hour using a high precision peristaltic pump (IsmaTec®) and Tygon tubing. The base of each FTR contained a 0.45  $\mu\text{m}$  filter (nitrocellulose membrane, Millipore) followed by a mesh screen to evenly distribute the influent and avoid channelization in the sediment core. The solution passed through a second 0.45  $\mu\text{m}$  filter and mesh screen before exiting the FTR (Figure 2). The effluent was transported through a PEEK™ flow cell (Luther et al., 2008), which contains a port that could be fitted with a mercury/gold microelectrode and a counter and reference electrode for in-line voltammetric measurements of  $\text{O}_2$ ,  $\text{Fe}^{2+}$ ,  $\text{Mn}^{2+}$ , and  $\sum\text{H}_2\text{S}$ . After exiting the PEEK™ flow cells, the effluent was collected in 15 mL polypropylene centrifuge tubes (Falcon®). Samples were collected with a frequency of 12 hours and alternately frozen or acidified with trace metal grade  $\text{HNO}_3$  (Fisher) to preserve for later analysis. For the anoxic phase of this experiment, the reactors were placed in an anaerobic chamber containing an ultra-high purity (UHP) atmosphere comprised of 85%  $\text{N}_2$ , 10%  $\text{CO}_2$ , and 5%  $\text{H}_2$ . All input solutions were degassed with UHP  $\text{N}_2$ . At the end of the incubation, the cores from each

reactor were sectioned into 0.5 cm sections for the first 2 cm, and 1 cm sections for the remaining 10 cm (14 sections per core). Each section was sub- divided into 3 fractions for triplicate analyses and extracted using the modified sequential extraction procedure of Tessier to determine the speciation of uranium and phosphate in the solid phase. The extraction procedure was also applied to the original soil (in triplicate) to determine the original speciation of uranium in these soils. The extracted solutions were filtered (0.22  $\mu\text{m}$ , nitrocellulose membrane, Millipore) and measured for uranium by ICP-MS.

To supplement the FTR study, batch adsorption experiments were conducted on unaltered Area 3 soils to elucidate any purely chemical processes effecting the removal of uranium within the reactors. Approximately 0.1 g of soil from Oak Ridge soil FWB120-06-48 was added to 30 mL simulated groundwater solution (Table 1) containing 40  $\mu\text{M}$  uranyl acetate in 50 mL centrifuge tubes. The pH was adjusted with either 1 M HCl or 1 M NaOH to achieve a range of values from 1 to 10. Each sample was equilibrated for 48 hours on a rotary wheel, then centrifuged and filtered (0.2  $\mu\text{m}$ , Millipore). The supernatant was measured for total uranium concentration by ICP-MS.

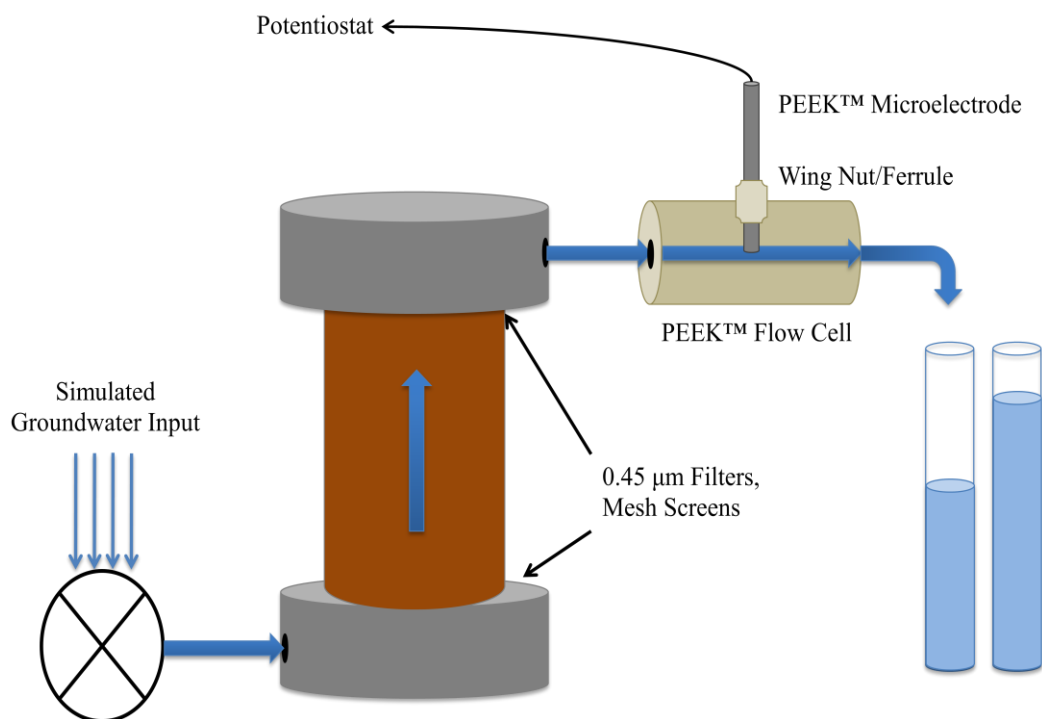


Figure 2. Schematic of the Flow Through Reactor set-up. Four reactors were used during this experiment. Blue arrows indicate simulated groundwater flow path. Reactors were incubated in an anaerobic chamber for the anoxic phase of the experiment.

Table 1. Composition of the simulated groundwater used in this study that reflects the geochemical conditions of Area 3 at the Oak Ridge Field Research Center, Oak Ridge (TN) (Beazley et al., 2011). All chemicals were reagent grade and prepared in MilliQ water (Barnstead).

Species	Concentration
$\text{Ca}(\text{NO}_3)_2$	202 $\mu\text{M}$
$\text{Fe}(\text{SO}_4)$	2.02 $\mu\text{M}$
$\text{MnCl}_2$	5.06 $\mu\text{M}$
KCl	402 $\mu\text{M}$
$\text{Na}_2\text{MoO}_4$	8.03 $\mu\text{M}$
$\text{MgSO}_4$	808 $\mu\text{M}$
$\text{NaNO}_3$	7.52 mM
$\text{KNO}_3$	7.5 mM



### **2.1.2 Timeline of changes to groundwater conditions**

The soils were first flushed with simulated groundwater (Table 1) buffered at pH 5.5 with MES in an aerobic environment for 70 days to raise the pH of the soil from 4.5 to 5.5 and monitor any natural respiration processes that could be occurring. The reactors were then placed in an anaerobic chamber under an 85% N<sub>2</sub>, 10% CO<sub>2</sub>, and 10% H<sub>2</sub> atmosphere. The input solution was degassed with UHP N<sub>2</sub>, and oxygen levels monitored by voltammetry using PEEK<sup>™</sup> flow cells. After 10 days all reactors were amended with an organophosphate source, glycerol-2 phosphate (G2P) (Sigma Aldrich), to stimulate the phosphatase activity of natural microbial communities. Three of the reactors denoted “Long Term G2P Amended Reactors” were amended with 20 mM G2P for 108 days, while the last one was only exposed to G2P for 10 days. In the next step, a solution of 200 µM uranyl acetate (Sigma) was continuously added to the reactors for 110 days to evaluate the effect of uranium on the stimulation of phosphatase activity by natural microbial communities. G2P was removed 12 days before uranium in the long term G2P reactors. The reactors were allowed to run 66 more days under anaerobic conditions before being transferred to aerobic conditions for an additional 30 days to reoxidize any uranium eventually precipitated by reduction. A summary of changes made to the input solution and redox state of the experiment over the duration of the FTR incubation is illustrated in Figure 3.

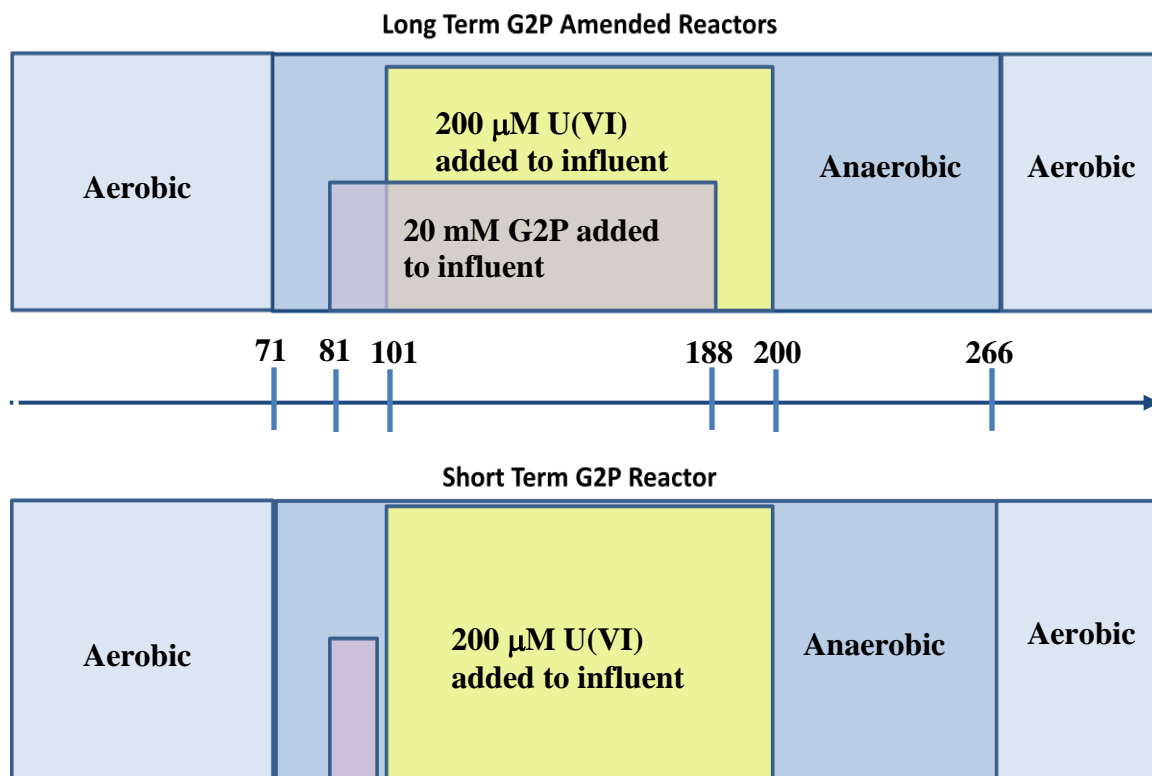


Figure 3. Timeline of the Flow Through Reactor study showing the oxidation state and different amendments made to the reactors. The long-term G2P amended reactors were run in triplicate.

## 2.3 Analytical Methods

### 2.3.1 Colorimetry

#### 2.3.1.1 Phosphate

Total free phosphate ( $\Sigma\text{PO}_4^{3-}$ ) was measured on a Milton Roy Spectronic, Model 501 spectrophotometer using the molybdate blue method (Murphy and Riley, 1962). Each sample was diluted 1000 x with MilliQ water to be within the range of the standards (0-25  $\mu\text{M}$   $\text{Na}_2\text{HPO}_4$ ). Standards were prepared in the same matrix as the samples. The reagents used were freshly made of 0.3 M ascorbic acid, 4.2 mM potassium antimony, 2.8 M  $\text{H}_2\text{SO}_4$  and 23 mM  $\text{NH}_4\text{-Mo}$ , all from trace metal grade salts. Color was allowed to develop for 15 minutes after adding the reagent mixture to the standards and samples. The samples were analyzed at 885 nm using a 1 cm cell. Molar extinction coefficients ( $\epsilon$ ) varied slightly depending on the solution matrix and ranged from 15,000 to 19,000  $\text{M}^{-1}\text{-cm}^{-1}$ .

#### 2.3.1.2 Nitrite

Nitrite was measured according to the azo dye method on a Milton Roy Spectronic, Model 501 (Grasshoff, 1983). Standards (0-10  $\mu\text{M}$ ) were made from anhydrous reagent grade  $\text{NaNO}_2$  in simulated groundwater diluted 100x with MilliQ water. The reagents consisted of separate solutions of 58 mM sulfanilamide ( $\text{C}_6\text{H}_8\text{N}_2\text{O}_2\text{S}$ ) in 10% HCl and 3.86 mM N-(1-Naphthyl)ethylenediamine dihydrochloride (NED) in MilliQ water. An aliquot of 20  $\mu\text{L}$  of the sulfanilamide was added to 1 mL of standard or sample and allowed to equilibrate for 1 minute, followed by the addition of

20  $\mu\text{L}$  of NED. Color was allowed to develop for 15 minutes before absorbance was measured at 540 nm using a 1 cm cell. The molar extinction coefficient ( $\epsilon$ ) was approximately  $37,000 \text{ M}^{-1}\text{-cm}^{-1}$ .

### **2.3.2 Inductively-Coupled Plasma Mass Spectrometry (ICP-MS)**

An Agilent 7500a Series system was used to measure total dissolved uranium concentrations. Samples and standards were prepared in 2% trace metal grade nitric acid (Fisher) matrix containing 500 ng/L holmium (SPEX CertiPrep) as internal standard to correct for the instrumental drift (Figure 4). Standard concentrations ranged from 0 to 16.8 nM and calibration curves were measured every 50 samples. River Water Certified Reference Material for Trace Metals (SLRS-5, National Research Council Canada, Ottawa, Canada) was used as a quality control sample to assess instrument and standard concentration accuracy. SLRS-5 and blank samples were measured every 10 samples (Figure 4). Typical minimum detection limit for uranium was 0.03 nM. Measured SLRS-5 values were within 10% of the certified value of 0.42 nM.

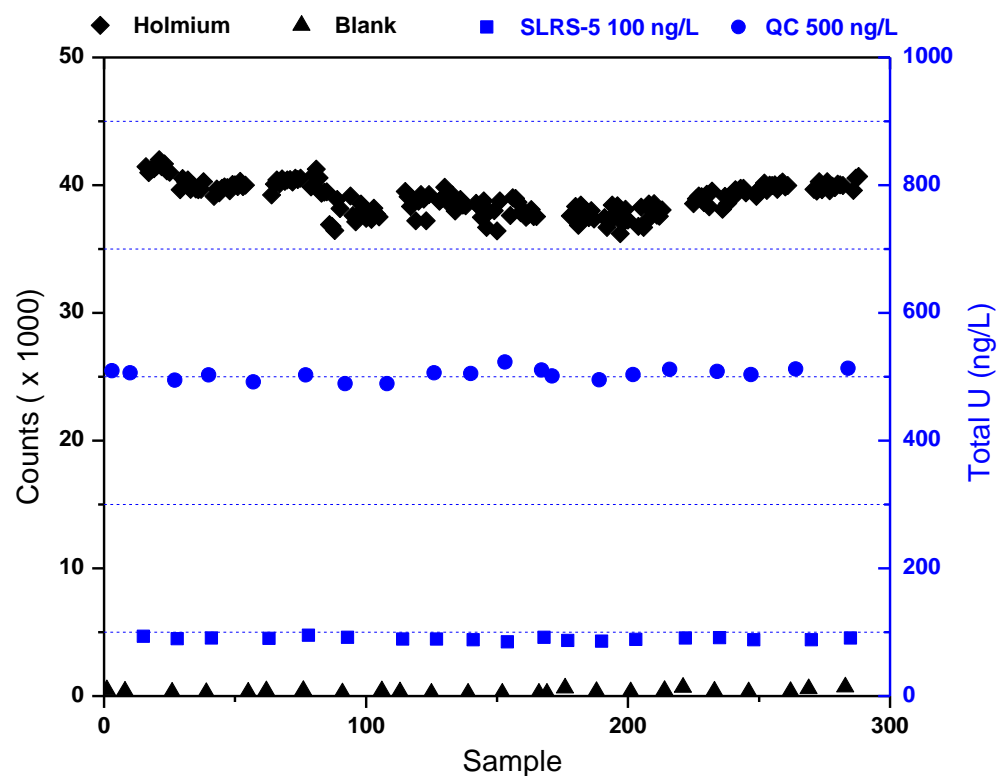


Figure 4. ICP-MS detector counts of internal standard and quality control samples (SLRS-5 and calibration blank) over the duration of a typical analysis for total dissolved uranium. SLRS-5 Certified material and quality control standards confirm that the analysis is accurate when the internal standard correction for instrument drift is applied to each sample.

### 2.3.3 Ion Chromatography

The measurements of bromide ( $\text{Br}^-$ ), nitrate ( $\text{NO}_3^-$ ), sulfate ( $\text{SO}_4^{2-}$ ), and G2P were conducted by Ion Chromatography using a Dionex GP50 gradient pump equipped with a Dionex 300 series conductivity detector and a computer-controlled Analytical Instrument Systems, Inc. (AIS, Inc.) LCC-100 integrator. A Dionex IonPac AS14A anion exchange column with guard column was used to separate the anions using a 1 mM  $\text{NaHCO}_3$  and 8 mM  $\text{Na}_2\text{CO}_3$  buffer containing 10% acetonitrile at a flow rate of 1 mL/min. After separation, the sample were passed through a Dionex AMMS 300 suppressor fed with a regenerant solution (25.8 mM  $\text{H}_2\text{SO}_4$ ) to neutralize the conductivity of the eluent. A typical chromatogram of all the species analyzed in this study shows good separation of the different anions, though G2P and phosphate peaks had to be deconvoluted using Peakfit (Jandel, Inc.) (Figure 5). Standards were prepared in the range of 0-2 mM, and samples were diluted 10 x in MilliQ water.

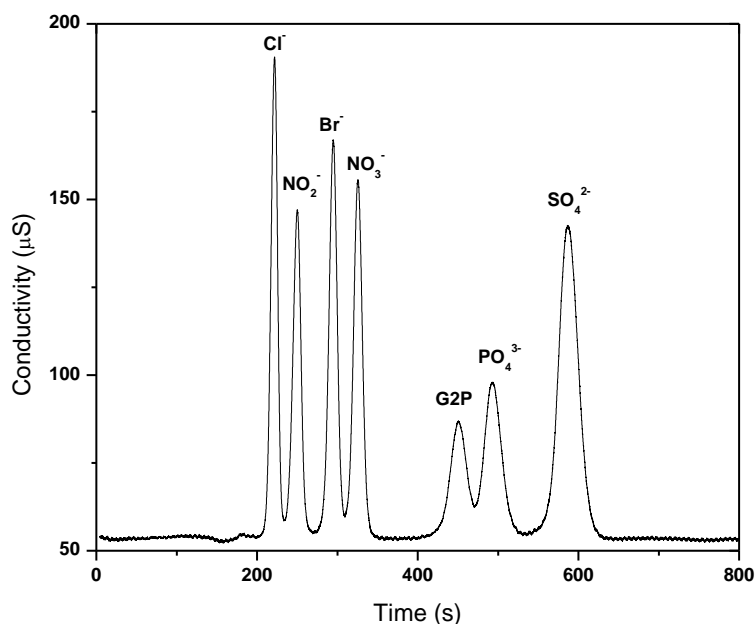


Figure 5. Ion chromatogram acquired in the presence of 1 mM  $\text{Cl}^-$ ,  $\text{NO}_2^-$ ,  $\text{Br}^-$ ,  $\text{NO}_3^-$ , G2P,  $\text{PO}_4^{3-}$  and  $\text{SO}_4^{2-}$ .

### 2.3.4 Voltammetry

Solid-state Au/Hg microelectrodes were used for the voltammetric measurements of  $O_2$ ,  $Fe^{2+}$ ,  $Mn^{2+}$ , and  $\Sigma H_2S$  (Brendel and Luther, 1995). The electrode consisted of a 100  $\mu m$  gold wire within  $\frac{1}{8}$  in. PEEK™ tubing, connected by copper wire and BNC connector to a computer-controlled AIS, Inc. DLK-60 potentiostat. The tip of the gold wire was polished with 15, 6, 1, and  $\frac{1}{4}$   $\mu m$  diamond paste and plated with Hg in  $HgNO_3$  for 4 minutes at -0.1 V. The electrode was then conditioned at -9 V for ninety seconds to ensure a good connection between the mercury film and gold wire. Electrode quality was assessed by performing oxygen measurements using linear sweep voltammetry, and  $Mn^{2+}$  calibrations were obtained using cathodic square wave voltammetry in degassed simulated groundwater. The other species (i.e.  $Fe^{2+}$  and  $\Sigma H_2S$ .) were calibrated with the pilot ion method using  $Mn^{2+}$  as the pilot ion (Brendel and Luther, 1995).

Measurements were performed by applying a range of potentials between the Au/Hg (working) electrode and a Ag/AgCl reference electrode, with a platinum wire used as a counter electrode. Prior to measurement, a conditioning potential of -0.1 V for 10 s was applied to the working electrode to clean the surface of the mercury. Linear sweep voltammetry (LSV) was used for the measurement of  $O_2$ , starting from a potential of -0.1 V to an ending potential of -1.75 V at a scan rate of 200  $mVs^{-1}$ . Figure 6a shows an example of three  $O_2$  measurements. The second  $O_2$  peak is obscured by the presence of an electrochemical signal attributed to the presence of MES, which also increased the detection limit of  $Mn^{2+}$  from 15  $\mu M$  to 250  $\mu M$ , without affecting the detection of  $Fe^{2+}$  at -1.4 V (Figure 6b).

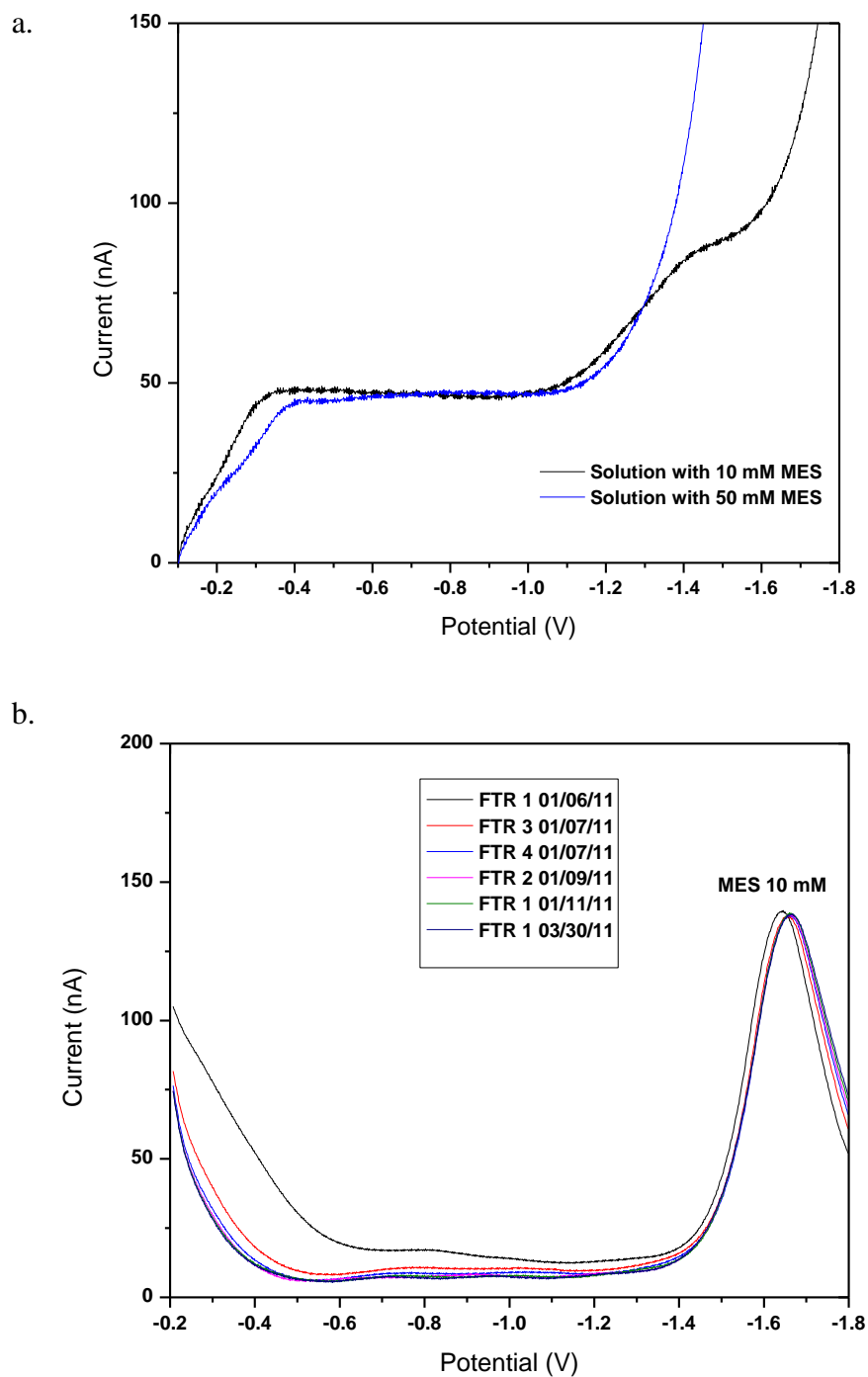


Figure 6. Typical examples of voltammograms obtained in-line in a flow through reactor to determine the concentration of (a) dissolved  $O_2$  by linear sweep voltammetry and (b) dissolved  $Fe^{2+}$  (MDL 10  $\mu M$ ),  $Mn^{2+}$  (MDL 250  $\mu M$ ), and  $\Sigma H_2S$  (MDL 0.2mM) by square wave voltammetry. The later species were never detected during these flow through incubations, even though the MES creates a peak at ca. -1.6 V that interferes with the  $Mn^{2+}$  measurement by increasing the minimum detection limit significantly.



## 2.4 Thermodynamic Calculations

The equilibrium modeling program MINEQL (Schecher et al. 2001) implemented with the two layer hydrous ferric oxide model of Dzombak and Morel (1990) was used to predict the adsorption of uranyl species on ORFRC soils assuming iron oxides as the main adsorbent. The model requires the user to input concentrations of species in solution and that of the hydrous ferric oxide. The adsorption model assumes that the iron oxide surface carries a set number of binding sites (determined by the concentration of total  $\text{Fe}^{3+}$ ), including 0.5% as strong binding and 20% as weak binding sites calculated by:

$$(1) \text{Fe(st)OH} = 0.005 \text{ mol/mol Fe} \times \text{Total Fe (mol/L)}$$

$$(2) \text{Fe(wk)OH} = 0.2 \text{ mol/mol Fe} \times \text{Total Fe (mol/L)}$$

The concentration of iron (25.8 g/kg) measured in soils from Area 3 of the OFRC (Barnett et al. 2002) along with the composition of the simulated groundwater (Table 1) were used in the model. The thermodynamic database was updated to include the most recent surface complexation constants for uranyl adsorption to both weak and strong sites (Waite et al. 1994). The system was maintained closed to the atmosphere and solids were not allowed to precipitate. The model was run as a pH titration, and the ionic strength was calculated at each iteration by the program.

## 2.5 One-dimensional Transient Reactive Transport Model

A one-dimensional advection-dispersion model (Eq.1) was used to determine the dispersion coefficient ( $D$ ), the advection rate ( $v$ ), and the retardation factor ( $R$ ) within the columns (Roychoudhury et al. 1998), using bromide breakthrough curves obtained in this study.

$$R \frac{dC}{dt} = D \frac{\partial^2 C}{\partial x^2} - v \frac{\partial C}{\partial x} \quad (\text{Eq. 1})$$

The analytical solution to the governing equation (Van Genuchten 1981) was used with an optimization procedure to calculate the three parameters. The optimization procedure, written in Matlab™, minimizes the difference between the data and the analytical solution of the differential equation to determine the three unknown parameters. The boundary conditions consistent with a flow-through column with continuous input of chemical species included:

$$C(x,0) = 0 \quad C(0,t) = C_0 \quad \frac{\partial}{\partial x} C(L,t) = 0 \quad (\text{Eq. 2})$$

where  $x$  is the spatial variable in the column,  $t$  is time,  $L$  is the total length of the column, and  $C_0$  is the input concentration of bromide.

The net production (positive) or consumption (negative) rates of phosphate, U(VI), G2P, nitrate, and nitrite were calculated by adding a reaction rate term to the right-hand side of Eq. 1. This net reaction rate represents the balance between the consumption and production rates of each species. These calculations were performed with the following boundary conditions to account for time periods during which some of

the species of interest were constantly injected into the columns and chemical changes were observed in the effluents of the columns:

$$C(x, t_0) = C_r \quad -D \frac{\partial C}{\partial x} + vC \Big|_{x=0} = vC_0 \quad \frac{\partial}{\partial x} C(L, t) = 0 \quad (\text{Eq. 3})$$

where  $t_0 \geq 0$  is the initial time selected to determine rates during a particular time period,  $C_r$  is the concentration of the species of interest across the column assuming that the concentration of the effluent is representative of the concentration in the columns, and all other parameters are the same as previously. The transport parameters calculated from the bromide breakthrough curves for three separate injections at days 1, 101, and 164 provided three different sets of transport parameters were used with the analytical solution to the governing equation (Van Genuchten 1981) to determine net reaction rates in each column by fitting the experimental data in Matlab™ using the least-squares optimization procedure described previously.

## **CHAPTER 3**

### **RESULTS**

The fate of aqueous uranium over the course of a 280 day flow through reactor incubation is analyzed in this study. Concentrations of conservative tracers, terminal electron acceptors, uranium, and products of microbial metabolism were monitored in the effluent for the duration of the experiment. To better understand uranium speciation in the solid phase, Tessier's sequential extraction technique was modified for uranium extraction. The incubated soils were extracted using the modified Tessier method upon completion of the incubation.

### 3.1 Results from the Modification of a Sequential Extraction Scheme

Modifications to the first step of Tessier's sequential extraction method targeting the loosely adsorbed phase involved lowering the pH of the leachate from 7 to 4.5 and adding either 10 mM sodium citrate or NTA to the 1 M  $\text{MgCl}_2$  (Figure 7). Lowering the pH of the 1 M  $\text{MgCl}_2$  from pH 7 to 4.5 did not change the amount of adsorbed uranium recovered. Washing the adsorbed uranium sample (Figure 7a) with the original 1 M  $\text{MgCl}_2$  solution at pH 4.5 and the same solution amended with 10 mM sodium citrate yielded around 30% of the total uranium in the sample. In contrast, the addition of 10 mM NTA to the 1 M  $\text{MgCl}_2$  increased the amount of total uranium recovered to around  $65 \pm 10\%$ . The majority of the remaining uranium ( $15 \pm 5\%$ ) was recovered by the slightly stronger NaOAc extractant.

The same extraction schemes were performed on a laboratory-synthesized uranyl phosphate precipitate (Figure 7b). The uranyl phosphate precipitate was not dissolved by any of the 1 M  $\text{MgCl}_2$  solutions, and the majority of the uranium (80-90%) was extracted from the mineral by washing with 1 M NaOAc at pH 5. Less than 10% of the total uranium was recovered in the following 1 M HCL extraction step, indicating that little uranium was left in the original sample after the second extraction step.

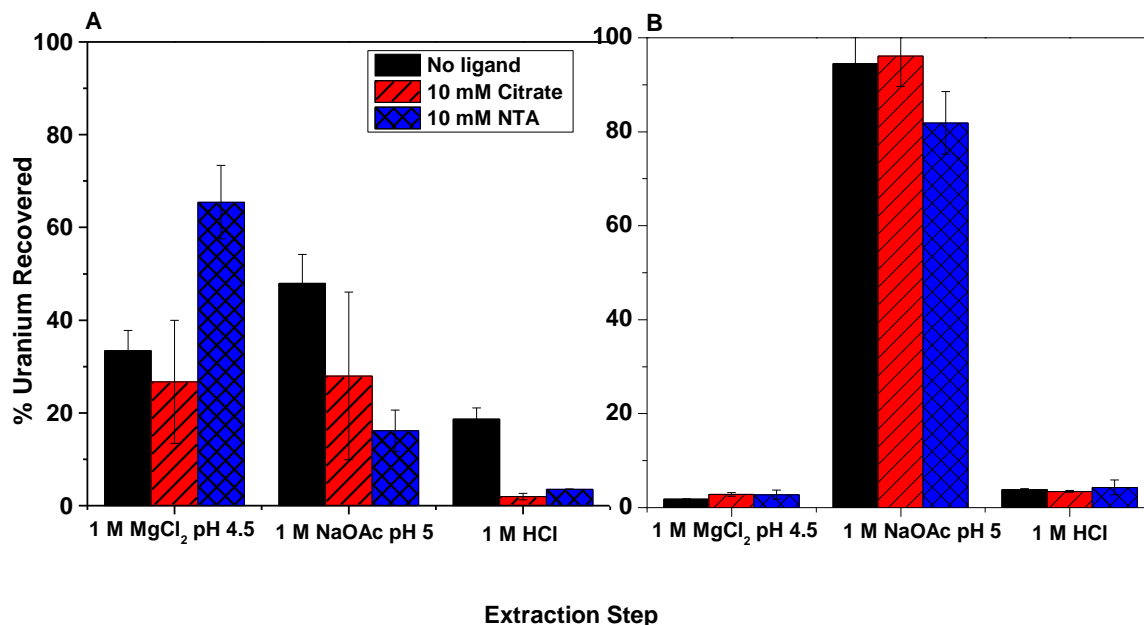


Figure 7 (A) Uranium adsorbed to lepidocrocite and (B) lab-synthesized uranyl phosphate precipitate extracted by the traditional Tessier method compared to a modification of the first step. Only the first step of the Tessier method was modified by adding either 10 mM NTA or Na-citrate. The pH of the first step was lowered from 7 to 4.5. Standard deviation represents variation on duplicate samples.

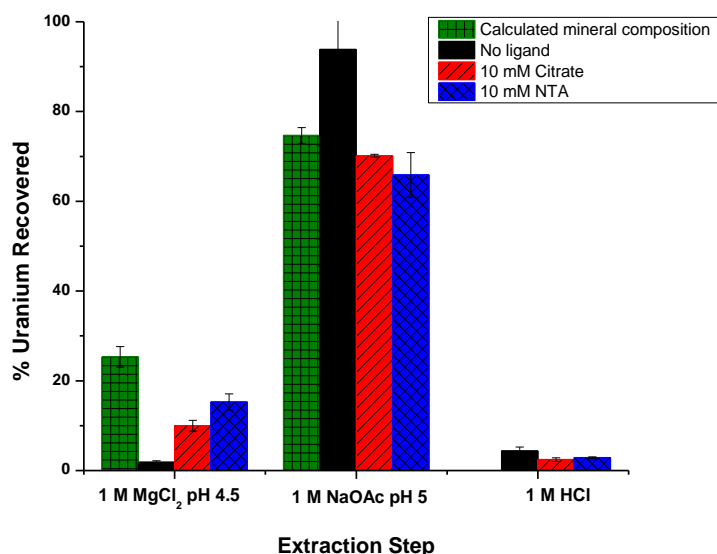


Figure 8. Solid phase mixture of uranium adsorbed to lepidocrocite and lab-synthesized uranyl phosphate precipitate extracted by the original Tessier method compared to a modification of the first step. The first bar represents the true percentage of uranium of the mineral/adsorbed iron oxide mixture. Standard deviation represents variation on duplicate samples.

Finally, a mixture of uranium adsorbed to lepidocrocite and uranyl phosphate precipitate underwent the same extraction schemes (Figure 8). The first bar in the figure of each extraction step represents the calculated percentages of adsorbed uranium (i.e. uranium that should be recovered in the first step) and uranium present as uranyl phosphate precipitate (uranium that should be recovered in the second step). When the original extraction method was used, almost no loosely adsorbed uranium was released by  $\text{MgCl}_2$ , and the majority of the uranium ( $> 90\%$ ) was extracted from the mixture by the NaOAc step. The addition of 10 mM sodium citrate or NTA increased the extraction of adsorbed uranium to 10% and 15% respectively in closer agreement with the calculated percentage of the mineral mixture (ca. 25%). None of the extraction schemes perfectly recovered the original mixture of adsorbed U(VI) and precipitated U(VI) phosphate; however, adding NTA to the first extractant solution increased the fraction of adsorbed uranium that was recovered.

## **3.2 Composition of the Effluent from Flow Through Reactor Incubations**

### **3.2.1 Bromide as a Conservative Tracer**

Bromide (10 mM) was injected into the flow through reactors intermittently during the incubation to determine the groundwater residence time and calculate the advection and dispersion coefficients used in the reactive transport model (Figure 9). Initial residence times varied from ca. 5 days in the short-term G2P amended reactor to ca. 15 days in the long-term G2P amended reactors (Figure 9). The second bromide injection began on day 101 and lasted 16 days. The residence times of all FTRs increased to 14 days for the short-term G2P amended reactor and some time greater than 16 days for the long-term G2P amended reactors (the tracer was not added over a long enough time period). Interestingly, the final bromide injection on day 164 revealed shorter residence times for all reactors (8 days) than the injection on day 101, with the exception of one of the long-term G2P amended reactors (20 days).



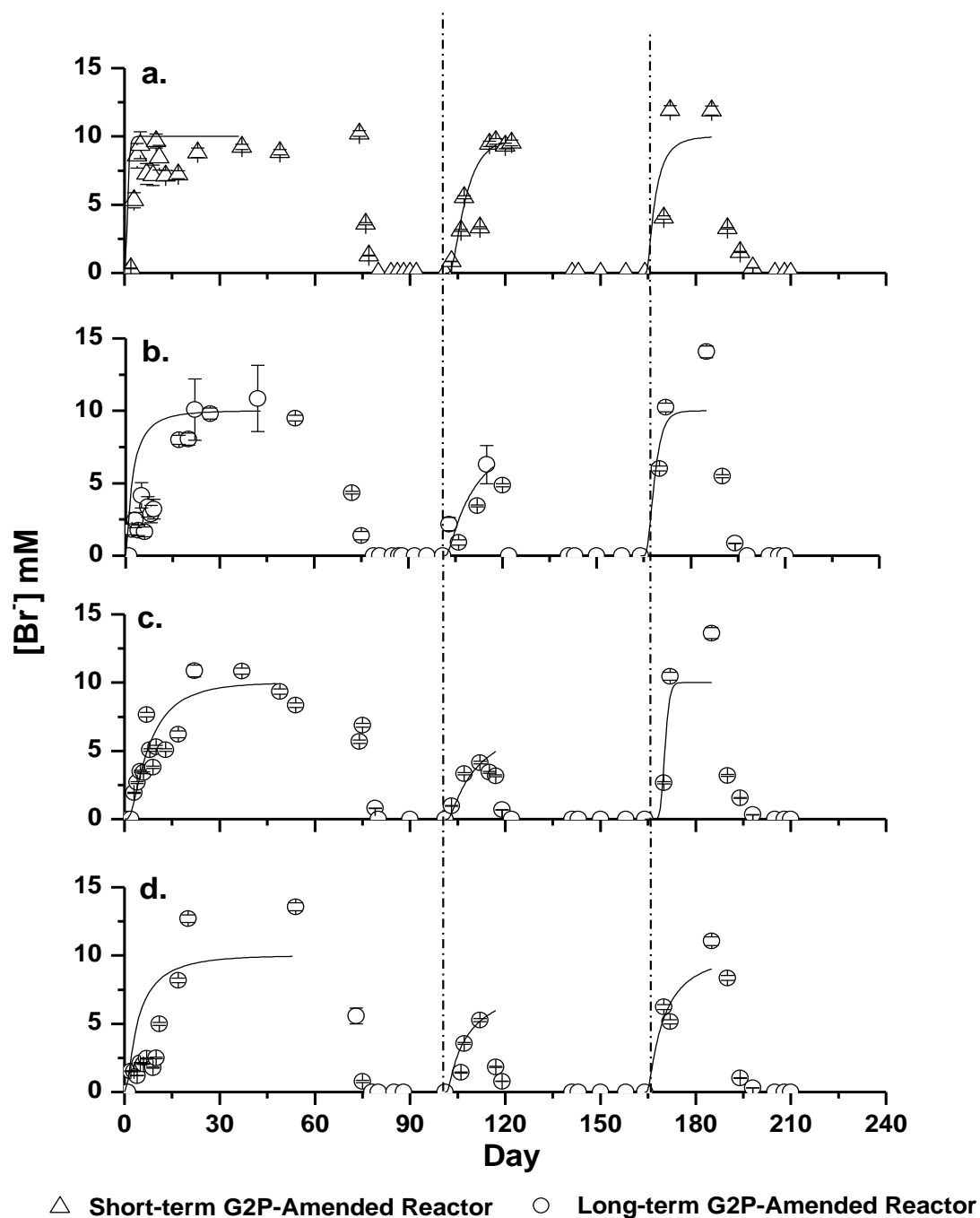


Figure 9. Effluent concentrations of bromide measured (symbols) and calculated from the transient 1D transport model (line) in the four FTRs over time during the incubation: a) short-term G2P amended reactor (triangles); and b) through d) the three long-term G2P amended reactors (circles). Bromide was added at days 0, 101, and 164 (101 and 164 indicated by vertical dashed lines). Error bars represent analytical error on the measurement in each reactor.

### 3.2.2 G2P Effect on Respiration Processes and Phosphate Production

Concentrations of terminal electron acceptors oxygen, nitrate, and sulfate as well reduced metabolites  $\text{Fe}^{2+}$ ,  $\text{Mn}^{2+}$ , and  $\Sigma\text{H}_2\text{S}$  were monitored over the duration of the incubations (Figure 10). Oxygen concentrations were maintained at saturation during the first 70 days of the incubation until the time it was removed from the feeding solution. Some nitrate consumption occurred during the initial aerobic phase of the experiment (days 0-70), as indicated by a decrease of approximately 5 mM nitrate in the effluent (Figure 10b). Nitrate consumption increased upon removal of oxygen from the feeding solution and, especially, upon introduction of G2P. In fact, the continuous input of 15 mM nitrate in the reactors was completely consumed for the duration of the G2P amendment in both the short (10 days) and long-term (108 days) G2P-amended reactors. Simultaneously, a short period of nitrite production ( $< 1.75$  mM) was stimulated in all the reactors (Figure 10b). When G2P was removed from the short-term reactor after 10 days, nitrate levels returned to the levels of the input solution (15 mM). The reactors amended with G2P for 108 days behaved similarly upon removal of G2P (Figure 10b). Sulfate concentrations varied slightly from the influent solution concentration but  $\Sigma\text{H}_2\text{S}$  was never detected in the effluent (data not shown). Similarly,  $\text{Fe}^{2+}$  and  $\text{Mn}^{2+}$  were never detected in the effluent over the duration of the experiment (data not shown), suggesting that iron and manganese reduction were not significant in these incubations.

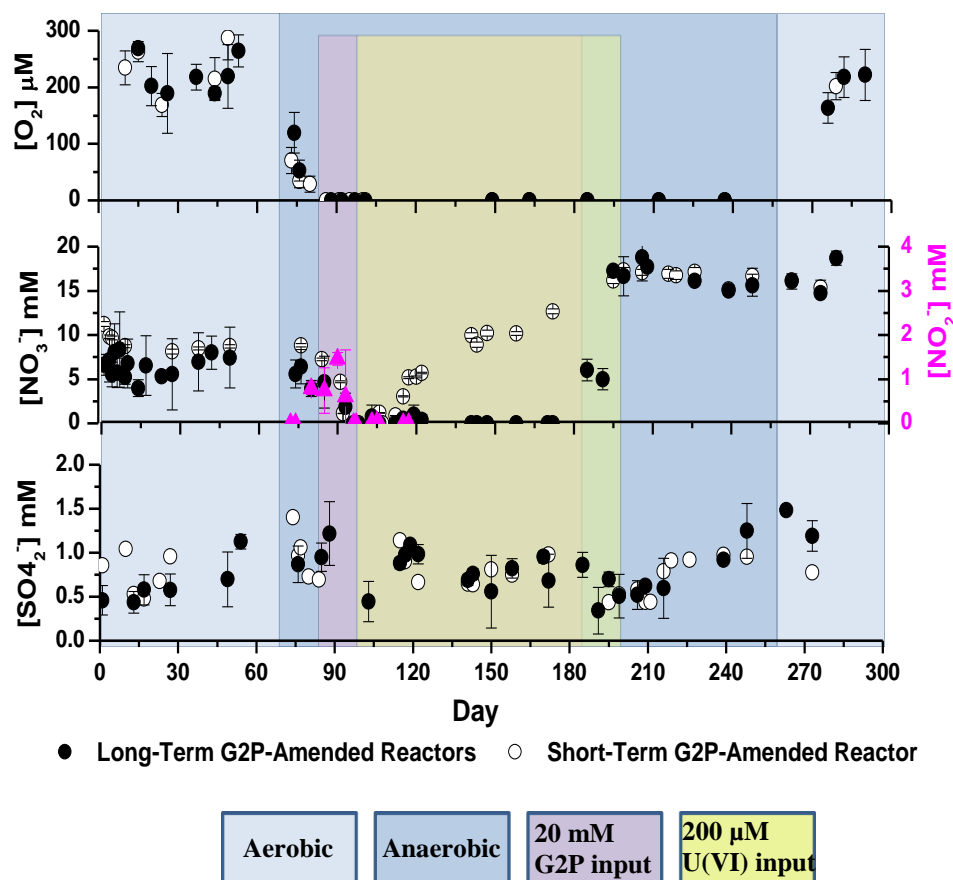


Figure 10. Average concentrations of oxygen, nitrate, nitrite, and sulfate in the three long term (black symbols) and the one short-term (open symbols) G2P amended reactors. Nitrite concentrations are represented by triangles. Error bars on solid symbols refer to the standard deviation of triplicate reactors. Error bars on open symbols refer to analytical error.

In addition to an increase in nitrate consumption, the addition of G2P to the influent coincided with the production of orthophosphates within the reactors. Phosphate concentrations reached as high as 10 mM in some reactors (Figure 11), suggesting that G2P was completely consumed during the incubations. Not surprisingly, production of phosphate ceased upon removal of G2P, and the concentration of phosphate decreased to below detection limit within 53 days after removal of G2P in the short-term amended reactor and 30 days for the long-term amended reactors.

### 3.2.3 Uranium Uptake by Flow Through Reactors

Uranium was not released significantly ( $< 20 \mu\text{M}$ ) from the Area 3 soils during the first 70 days of the incubations in aerobic conditions, the following 20 days in anaerobic conditions, or the few days during which G2P was injected in the reactors (Figure 11). These findings indicate that authigenic uranium is either incorporated in the soil matrix or eventually transformed from one solid phase to another during the incubations. A concentration of  $200 \mu\text{M}$  uranium was fed for 110 days to the short term G2P-amended reactor after G2P was removed from the input solution. In contrast, the long term G2P-amended reactors were fed G2P and uranium simultaneously for 100 days. During this time, uranium effluent concentrations between short and long term G2P reactors differed slightly. First, the concentration of aqueous uranium in the effluent of the short term G2P-amended reactor remained less than  $20 \mu\text{M}$  during the entire experiment even though  $200 \mu\text{M}$  U(VI) was injected in the reactors for 100 days (Figure 11). Interestingly, while the concentration of dissolved uranium remained low in the long term G2P-amended reactors, it increased from  $10$  to  $40 \mu\text{M}$  after 40 days of constant G2P input but then decreased to less than  $10 \mu\text{M}$  upon G2P removal. G2P addition in both short (10 day G2P amendment) and long-term (100 day G2P amendment) reactors coincided with an increase in effluent pH from 5.5 to 7 and 7.8, respectively (Figure 11). pH levels returned to 5.5 after G2P was removed from the input solution. These results suggest that the speciation of uranium may have been affected by the pH changes. Finally, re-introduction of oxygen in the reactors did not affect dissolved uranium concentrations in the effluent (Figure 11). These findings suggest either that uranium was

not reduced during the incubations or that reoxidation was followed by uptake in the solid phase.

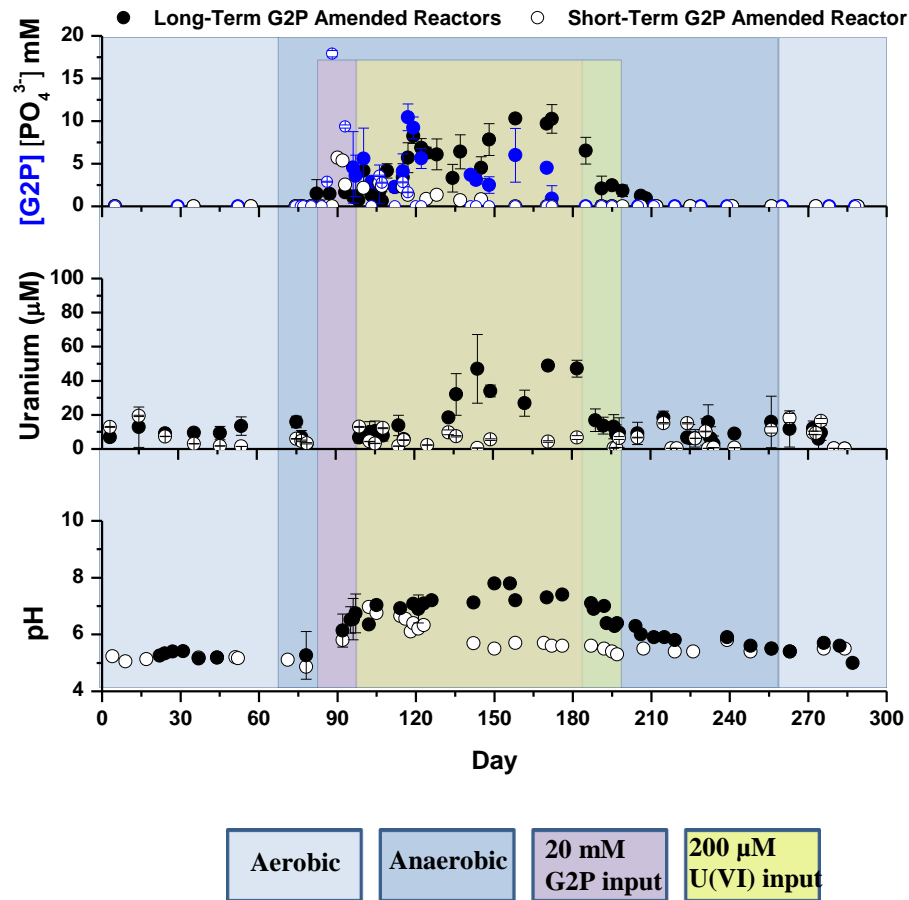


Figure 11. pH and concentration of G2P, total soluble phosphate, and uranium measured in the effluent of the 3 long-term G2P amended FTRs (closed symbols) and 1 short-term G2P amended FTR (open symbols). Blue symbols correspond to G2P measurements. Error bars on solid symbols refer to the standard deviation of triplicate reactors. Error bars on open symbols refer to analytical error.

### **3.2.4 Batch Adsorption Experiments**

Preliminary batch adsorption experiments were conducted on unmodified contaminated soil from Area 3 at Oak Ridge Field Research Center (ORFRC) to determine the competitive role of U(VI) adsorption in the biomineralization of U(VI) phosphate minerals. The results show that total dissolved uranium at equilibrium with Area 3 soils decreased from ca. 40  $\mu\text{M}$  at pH 4.5 to below detection limit at pH 7 (Figure 12). Dissolved uranium remained below detection limit from pH 7 to pH 10.5, indicating that adsorption completely removes at least 40  $\mu\text{M}$  uranium from solution in this pH region. Dissolved uranium levels increased with pH above pH 10.5, indicating that uranyl adsorption is not favored above that pH.

Dissolved U(VI) concentrations predicted by the equilibrium model assuming iron oxides as the main adsorbent fit the data well over the pH range studied, suggesting that the iron oxide content of the soil is controlling uranyl adsorption.

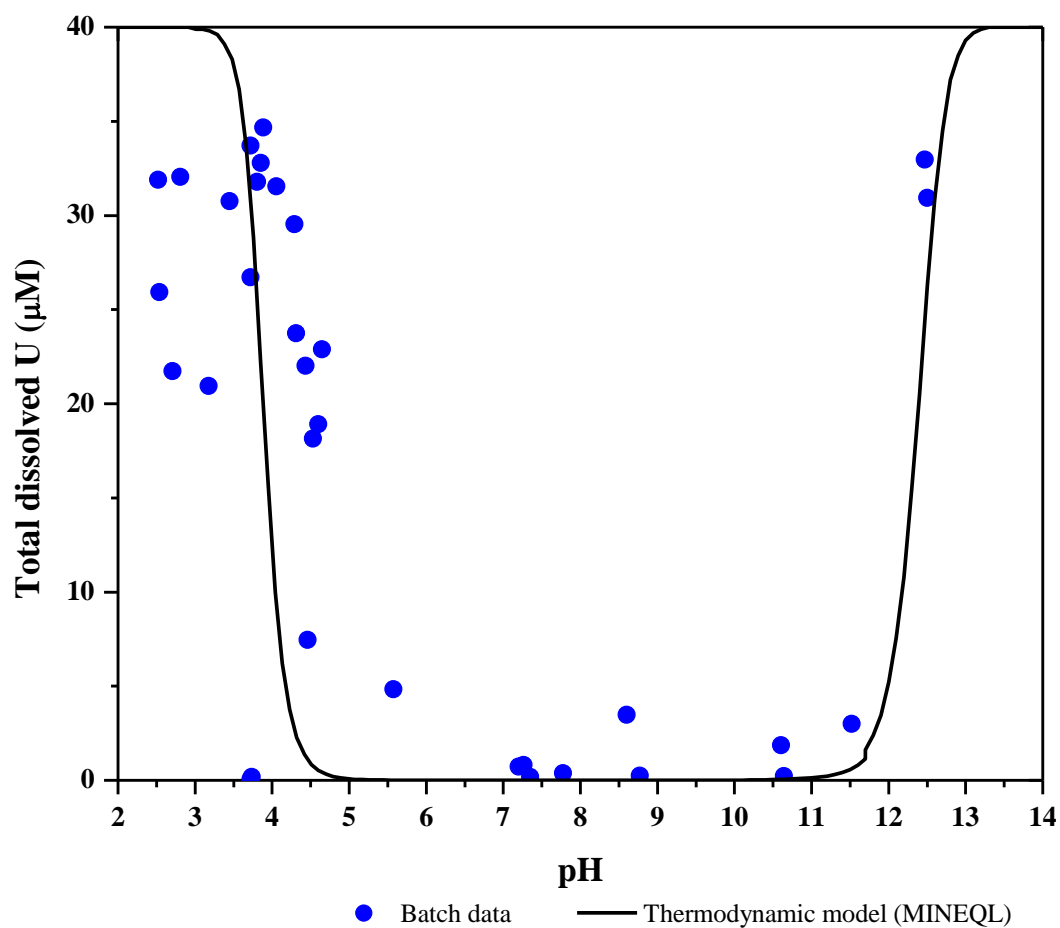


Figure 12. Uranium adsorption curve from batch experiments and a thermodynamic model that describes the adsorption process assuming iron oxides as the main adsorbent. Batch data represent single measurements; error bars of measurements are within symbol.

### 3.2.5 Sequential Extraction Scheme Applied to Flow Through Reactor Soils

Upon completion of the flow through reactor incubations, soils from each of the reactors were sectioned from the inlet into 0.5 cm slices for the first 2 cm, then 1 cm slices for the remaining 10 cm and sequentially extracted according to the modified Tessier scheme. Solid phase uranium was recovered predominantly in the first 2-3 cm of the FTRs (Figure 13). Uranium was not present in significant quantities in the loosely adsorbed fraction recovered by 1 M  $\text{MgCl}_2$ , 10 mM NTA, pH 4.5). In all four reactors, the highest quantity of solid phase uranium was recovered by the extractant targeting the uranyl phosphate/carbonate precipitates (1 M NaOAc). The short-term G2P amended reactor contained 4-6  $\mu\text{mole U/g}$  bound as uranyl phosphate/carbonate precipitates in the first 2 cm, while the long-term G2P amended reactors (FTRs 1, 3, and 4) showed recoveries of approximately 1-4  $\mu\text{mole U/g}$ . In these reactors (FTRs 1,3,4), the remaining fractions (bound to Fe/Mn oxides, bound to organic matter, and residual) were less than 1  $\mu\text{mole U/g}$ . In turn, 1-5  $\mu\text{mole U/g}$  associated with the fraction bound to Fe/Mn oxides was recovered in the first 2 cm of the short-term G2P amended reactor (FTR 2) (Figure 13).



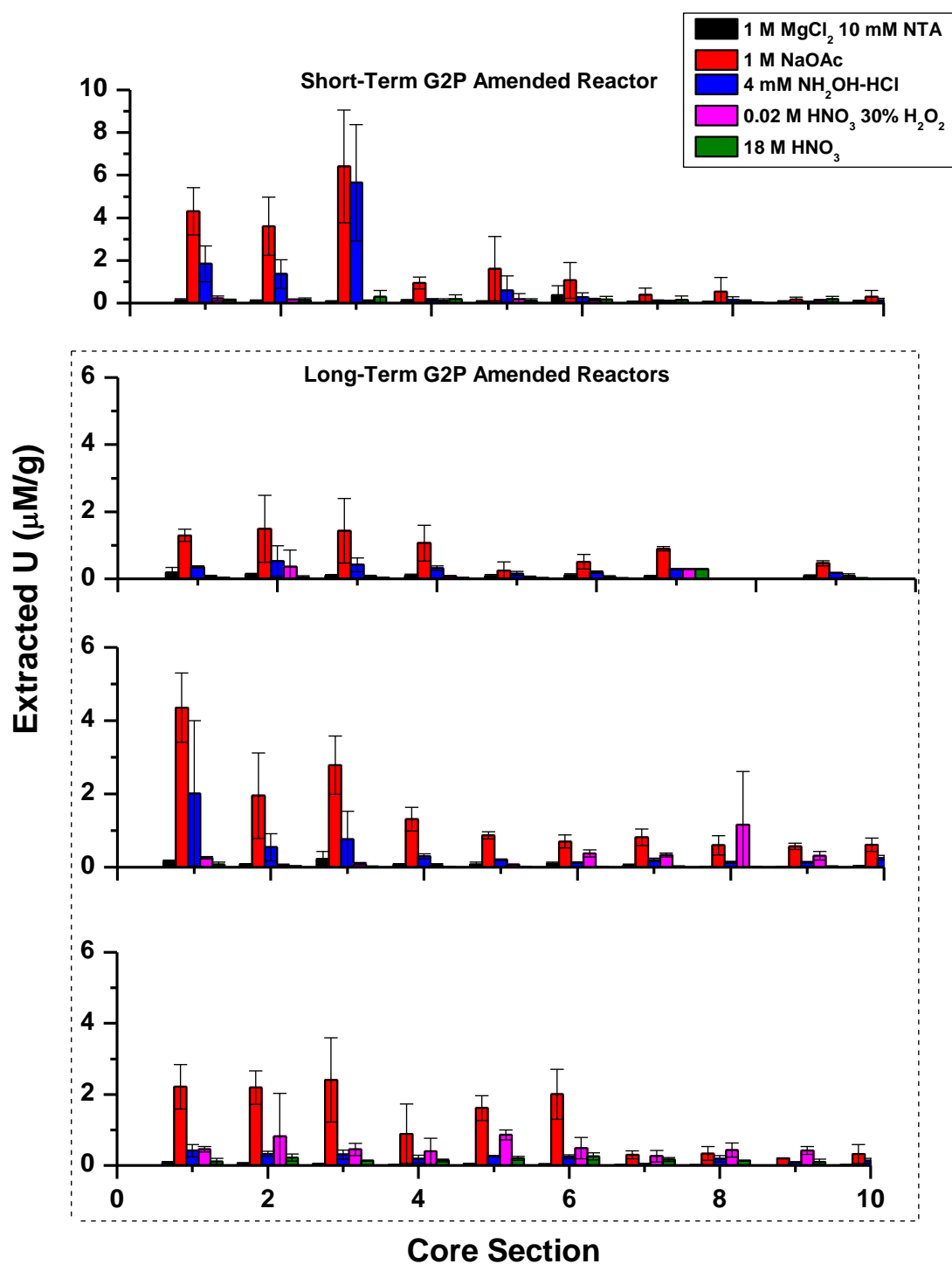


Figure 13. Total uranium recovered from Tessier's sequential extraction scheme performed on soils from the short (top) and long term G2P amended reactors after incubation with G2P and 200  $\mu\text{M}$  uranyl acetate. Error bars represent the results of triplicate samples. Note larger scale on short-term reactor graph.

## CHAPTER 4

### DISCUSSION

Uranium contaminations from nuclear materials processed at multiple sites across the country has lead to the development of new remediation strategies that could be implemented *in situ* at Department of Energy sites such as Oak Ridge, TN, Hanford, WA, and Rifle CO to minimize costs associated with current remediation strategies. The biomineralization of uranium phosphate minerals is a novel *in situ* remediation strategy that encourages the activity of the local microbial community to immobilize aqueous uranium over great distances in contaminated subsurfaces.

The biomineralization of uranium phosphate may occur both aerobically and anaerobically in pure cultures of bacteria previously isolated from a uranium-contaminated environment at Oak Ridge Field Research Center (Beazley et al. 2007; 2009). Simultaneously, the phosphatase activity of subsurface microbial communities may be stimulated in aerobic conditions by addition of a labile organophosphate compound in soils from the same site (Beazley et al. 2011). While this remediation technique has successfully removed uranium in heterogeneous soil columns under aerobic conditions, further studies were needed to access its viability under anaerobic conditions. In this study, the feasibility of using *in situ* biomineralization as a remediation strategy was tested under anaerobic conditions using low pH soils from a uranium-contaminated site at Oak Ridge Field Research Center. Flow-through reactors (FTRs) were used to determine if natural microbial phosphatase activity in soils from the ORFRC could efficiently remove aqueous uranium in anaerobic conditions and

outcompete uranium reduction and adsorption onto the solid phase. The information gained from this small-scale study may provide insights on the application of the biomineralization of uranium phosphate minerals as a bioremediation strategy for an actual site.

FTRs have been used extensively to investigate and model a variety of biogeochemical reactions (Roychoudhury et al. 1998; Carey et al. 2005; Pallud et al. 2007; Beazley et al. 2011). They are useful for this type of study as they provide a way to investigate the response of an entire microbial community to changing groundwater conditions. Additionally, FTRs may help to study competitive reactions in soils and sediments and prevent the accumulation of reaction products in batch reactors that could influence biogeochemical reactions.

A groundwater solution mimicking current conditions at ORFRC was pumped vertically through reactors containing soils from ORFRC. After a 2 month equilibration period under aerobic conditions, Glycerol-2 phosphate (G2P) was added to the influent under anaerobic conditions to assess the ability of indigenous microbes to hydrolyze an organophosphate source and possibly stimulate anaerobic respiration. Additionally, aqueous uranium was pumped through the reactors to investigate the fate of uranium in the soils. Specific uranium removal processes were analyzed by a combination of batch adsorption studies on the original soil, equilibrium adsorption models, a kinetic analysis of the data obtained with the FTRs, and a modified sequential extraction scheme applied to the solid phase at the end of the incubations. Finally, the stability of the immobilized uranium was tested by returning the columns to aerobic conditions.

#### 4.1 Modified Sequential Extraction Scheme

In preparation for the solid phase extraction used to determine the speciation of uranium in contaminated soils, Tessier's sequential extraction method for the speciation of trace metals (Tessier et al. 1979) was applied to simple solid phase mixtures to better understand how the operationally-defined procedure is able to distinguish U(VI) adsorbed to the soils and uranyl phosphate precipitates. Although Tessier's method is widely used to extract trace metals in soils and sediments, common issues such as readsorption and redistribution of the extracted trace metals onto the remaining solid phase has been shown to occur, which can lead to errors in determining solid phase speciation (Shan et al. 1993). Previous studies performed on radionuclide fractionation in soils revealed that the speciation of radionuclides varied depending on the extraction method performed and the species studied (Shan et al. 1993; Schultz et al. 1998; Blanco et al. 2004). More recent extraction experiments performed on ORFRC soils showed that Tessier's original method does not completely recover adsorbed U(VI) (Beazley et al. 2011). It was therefore hypothesized that the pH of the first extraction step, which should release loosely-adsorbed U(VI) using an ion exchange process with 1 M  $\text{MgCl}_2$  at pH 7, could contribute to the incomplete recovery of uranium either by re-precipitation of a uranium phase in solution or resistance to ion exchange by  $\text{Mg}^{2+}$ . Indeed control experiments with iron oxides and thermodynamic calculations predict uranium adsorption to be most efficient and the mineral metaschoepite ( $(\text{UO}_3) \cdot 2(\text{H}_2\text{O})$ ) to precipitate at circumneutral pH. Previously, this artifact was avoided by lowering the pH of the first extraction step from 7 to 5 (Schultz et al. 1998). In the present study, however, lowering the pH of the  $\text{MgCl}_2$  extraction step to 4.5 in control experiments did not increase the recovery of

freshly adsorbed U(VI) significantly, as approximately 35% of the adsorbed U(VI) was recovered by the  $\text{MgCl}_2$  step, while the remainder was recovered by the 1 M NaOAc extraction step (Figure 7 a) which is supposed to target mineral carbonate and phosphate precipitates (Tessier et al., 1979).

To further increase recovery of the loosely adsorbed U(VI), it was hypothesized that strong organic ligands could be used in rinses between extracting steps; however, no significant increase in the extraction of adsorbed uranium was observed in the presence of EDTA as strong ligand of U(VI) (Schultz et al. 1998). Other strong complexing agents, such as citric acid and NTA have been shown to alter the sorption and reductive precipitation behavior of uranium by keeping it in solution (Haas et al. 2004; Suzuki et al. 2010). As extractions conducted at pH 4.5 did not extract uranyl phosphate precipitates (Figure 6 b) and as both NTA and citrate form thermodynamically stable aqueous complexes with U(VI) at that pH (Stary et al. 1961; Smith et al. 2003) these two modifications of the first extraction step of the Tessier method were tested in the present study. Addition of 10 mM NTA increased adsorbed U(VI) recovery to ca. 70% and did not significantly target the uranyl phosphate precipitate (Figure 7 a and b), suggesting indeed that re-precipitation of metaschoepite in non-complexation media was probably responsible for the poor recovery of the loosely-adsorbed uranium at pH 7 and 4.5 without external ligand addition. In turn, citrate did not significantly enhance adsorbed U(VI) extraction, probably because the complexes formed with U(VI) are not strong enough to compete with hydrolysis. Citrate tends to form dimers with the uranyl ion at low pH (Allen et al. 1996) while NTA forms tridentate complexes with uranyl ions metals which enhances stabilization (Teleb et al. 2005). To further test the recovery of the

modified scheme, a mixture with a known amounts of adsorbed U(VI) and uranyl phosphate precipitates were extracted using the modified ion-exchange step. Although adsorbed U(VI) recovery (66%) was lower than predicted in the mixture, the presence of NTA recovered a higher amount of the adsorbed U(VI) fraction without dissolving the uranyl phosphate precipitate (Figure 8). This modification was therefore adopted for the soil extractions used in the rest of this thesis.

#### **4.2 Transport Parameters Calculated from Inert Tracer**

Transport parameters were calculated using an inert tracer ( $\text{Br}^-$ ) to investigate whether porosity changes that could occur by the precipitation of uranium phosphate minerals affected the transport of solutes in the reactors (Table 2). The advection and dispersion coefficients did not vary significantly over the course of the incubation in the long-term G2P amended reactors (Table 2). This could be due to the error associated with varied transport behavior between the 3 separate reactors. The short-term G2P amended reactor, however, displayed a marked decrease in the dispersion and advection coefficients from days 1 to 101. The dispersion decreased by a factor of 10, and the advection coefficient decreased by a factor of 4 (Table 2). The change in soil porosity could be due to the formation of uranyl phosphate precipitates after the addition of uranium on day 101. The final transport parameters calculated after day 164 show a decrease in dispersion (from  $7.7$  to  $2.5 \times 10^{-5} \text{ cm}^2 \text{ sec}^{-1}$ ) and a slight increase in the advection rate (from  $1.1$  to  $2.4 \times 10^{-5} \text{ cm sec}^{-1}$ ), indicating small changes in the porosity of the soil associated with the change in redox potential.

Table 2. Average transport parameters calculated by a one-dimensional advection dispersion model of the average bromide concentrations in the effluent of the long-term and short-term G2P amended reactors. Standard deviations for the long-term G2P amended reactors correspond to variations in triplicate reactors.

Reactor	Day	Retardation Factor (R)	Dispersion Coefficient (D) (cm <sup>2</sup> sec <sup>-1</sup> )	Advection Rate (v) (cm sec <sup>-1</sup> )
Long Term G2P-Amended (3)	1-100	1	6.3 (±8) x 10 <sup>-5</sup>	0.97 (±2.3) x 10 <sup>-5</sup>
	101-163	1	9.1 (±7.5) x 10 <sup>-5</sup>	0.43 (±5.5) x 10 <sup>-5</sup>
	164-288	1	9.6 (±3.4) x 10 <sup>-5</sup>	1.9 (±5.4) x 10 <sup>-5</sup>
Short Term G2P-Amended	1-100	1	40 x 10 <sup>-5</sup>	4 x 10 <sup>-5</sup>
	101-163	1	7.7 x 10 <sup>-5</sup>	1.1 x 10 <sup>-5</sup>
	164-288	1	2.5 x 10 <sup>-5</sup>	2.4 x 10 <sup>-5</sup>

### 4.3 Respiration Processes in Anaerobic ORFRC Soils

Nitrate was partially consumed during the aerobic phase of the FTR experiment suggesting as proposed previously (Beazley et al. 2011) that small anaerobic zones coexist with aerobic conditions within the soil column. The high and sudden consumption of nitrate, temporary production of nitrite upon introduction of G2P in the reactors (Figure 10), and lack of dissolved  $\text{Fe}^{2+}$  and  $\text{Mn}^{2+}$ , as well as thiosulfate, elemental sulfur, or polysulfides at the output of the FTRs indicate that nitrate reduction became the dominant respiration pathway once oxygen was removed from the input solution. Indeed, nitrate concentrations in groundwater of Area 3 at the ORFRC are high enough to offer an abundant source of the more thermodynamically favorable terminal electron acceptor (Brooks et al., 2001).

Net reaction rates for nitrate removal determined from the one dimensional reactive transport model were strongly affected by G2P introduction. Average nitrate consumption rates increased from  $0.61 \pm 0.45 \text{ mM d}^{-1}$  to  $1.6 \pm 0.74 \text{ mM d}^{-1}$  in the three long-term G2P-amended reactors upon G2P addition on day 81 (Table 3). A similar increase in the consumption rate ( $0.49$  to  $1.6 \text{ mM d}^{-1}$ ) occurred in the short-term G2P-amended reactor (Table 3). On day 93, however, when G2P was removed from the input solution of the short-term G2P amended reactor, nitrate consumption decreased from  $1.6$  to  $0.32 \text{ mM d}^{-1}$ , while the long-term G2P amended reactors reached even higher levels of nitrate consumption ( $1.7 \pm 0.74 \text{ mM d}^{-1}$ ) over the next 106 days. On day 188, G2P was removed from the input of the long-term G2P amended reactors, and nitrate consumption rates decreased to  $0 \text{ mM d}^{-1}$ . At this point, the short-term G2P amended reactor also displayed a negligible nitrate consumption rate (Table 3). These findings suggest that



nitrate reduction is catalyzed by G2P, though it is not clear whether G2P is hydrolyzed for phosphorus requirements or used as carbon source. The widespread nitrate contamination at the ORFRC creates favorable conditions for nitrate reduction or denitrification, as well as the potential for some of these microorganisms to display phosphatase activity. Microbes capable of denitrification or nitrate reduction have been identified in ORFRC soils and groundwater (Waldron et al. 2009; Spain et al. 2011), and the bacterium *Rahnella* Y9602, isolated from ORFRC soils, has been shown to hydrolyze organic phosphate using Glycerol-3 phosphate (G3P) as a carbon and phosphorus source under anaerobic conditions with nitrate as a terminal electron acceptor (Beazley et al. 2009). In a separate aerobic pure culture studies, microbes isolated from ORFRC including *Aeromonas hydrophila* M1, *Pantoea agglomerans* N51, and *Pseudomonas rhodesiae* O25 all displayed the ability to hydrolyze G3P and precipitate uranium phosphate minerals (Shelobolina et al. 2009). Another flow through reactor incubation using Area 3 soils from the ORFRC showed that the natural microbial community was able to hydrolyze G2P aerobically, though nitrate reduction was found to occur simultaneously in small anaerobic microniches within the reactors (Beazley et al. 2011).

The soils in this experiment and that of Beazley and colleagues (2011) and the pure culture study with *Citrobacter* (Macaskie et al. 1994) used G2P as a combined carbon, phosphorus, and energy source as opposed to G3P. A study using *Citrobacter* showed that phosphatase activity decreased in the presence of glucose or glycerol, and that phosphatase activity was higher in “starved cells” upon introduction of G2P (Butler et al. 1991). The results suggest that the ability of microbes to utilize G2P or G3P as a

combined carbon and phosphorus source is controlled by the availability of a preferable carbon source.

Phosphate production coincided with nitrate consumption within the reactors (Figure 10, 11). Additionally, when G2P was removed from the short-term amended reactor, phosphate production and nitrate consumption rates both decreased substantially from 0.37 to 0.0036 mM d<sup>-1</sup>. The long-term G2P amended reactors continued to display higher rates of phosphate production ( $0.84 \pm 0.25$  mM d<sup>-1</sup>) for more than 30 days during the addition of G2P, but decreased to 0 mM d<sup>-1</sup> after G2P removal from the feeding solution (Table 3).

A slight increase in phosphate production rates in the long-term G2P amended reactors occurred after day 130 ( $0.84 \pm 0.25$  mM d<sup>-1</sup> to  $0.89 \pm 0.47$  mM d<sup>-1</sup>). The increase in phosphate production rate is likely attributed to the increase in pH from 5.5 to 7 that occurred during this time. A higher pH would cause the surface charge on the iron oxides present in the soil to become more negative, which could lead to the desorption of the negatively charged phosphate ion. The increase in pH could have caused an increase in the rate of G2P hydrolysis; however, G2P consumption rates did not change during this time.

Rates of G2P removal were higher than phosphate production rates in both long and short-term G2P amended reactors. In the short-term G2P amended reactor, G2P consumption was 1.7 mM d<sup>-1</sup> compared to 0.37 mM d<sup>-1</sup> of phosphate production. Long-term G2P amended reactors showed initial rates of G2P consumption of  $2.97 \pm 1.28$  mM d<sup>-1</sup> and  $0.25 \pm 0.22$  mM d<sup>-1</sup> phosphate production (Table 3). Upon uranium addition, G2P consumption rates decreased to  $-1.22 \pm 0.98$  mM d<sup>-1</sup> and phosphate production increased

to  $0.84 \pm 0.25 \text{ mM d}^{-1}$ . In all reactors, G2P was consumed at a higher rate than phosphate production according to the concentration of phosphate in the effluent. The missing phosphate could have been adsorbed or precipitated as minerals within the columns. Alternatively, the G2P could have been taken up by the columns through adsorption without undergoing hydrolysis.

Phosphate production in anaerobic conditions in the presence of G2P, suggests that a significant fraction of the microbial community had the ability to hydrolyze G2P using nitrate as a terminal electron acceptor. This is only the second report (after Beazley et al., 2011) that demonstrates the ability of the natural microbial community at the ORFRC to hydrolyze large concentrations of organophosphate.

Table 3. Net reaction rates for dissolved species in the flow through reactors (pH 5.5) determined by the one-dimensional reactive transport model. Consumption and production rates are indicated by negative and positive values, respectively.

Reactor	Days	$\text{NO}_3^-$ (mM d <sup>-1</sup> )	$\text{NO}_2^-$ (mM d <sup>-1</sup> )	$\text{PO}_4^{3-}$ (mM d <sup>-1</sup> )	G2P (mM d <sup>-1</sup> )	U(VI) ( $\mu\text{M d}^{-1}$ )
Short term G2P- Amended Reactor	1 - 70	-0.49	0	0	0	0
	71 - 80		0.13	0	0	0
	81 - 100	-1.6	0.33	0.37	-1.7	0
	101 - 187	0	-0.19	0.0036	-0.0015	-10
	188-200	0	0	0	0	-10
Reactor 1	1 - 70	-0.51	0	0	0	0
	71 - 80		0.67	0	0	0
	81 - 90	-0.69	0.098	0.5	-1.4	0
	90-100		-0.19			0
	101 - 130	-2.3	0	1	-0.37	-25.2
	130-187			1.4		
	188-200	0	0	0	0	-5.1
Reactor 3	1 - 70	-0.22	0	0	0	0
	71 - 80		0.89	0	0	0
	81 - 90	-1.8	0.16	0.11	-3.5	0
	90-100		-0.49			0
	101 - 130	-2	0	0.98	-2.3	-23.4
	130-187		0	0.46		
	188-200	0	0	0	0	-20.7
Reactor 4	1 - 70	-1.1	0	0	0	0
	71 - 80		0	0	0	0
	81 - 90	-2.2	0	0.13	-4	0
	90-100		0			0
	101 - 130	-0.9	0	0.55	-1	-11.7
	130-187		0	0.82		
	188-200	0	0	0	0	-11.7
Average Long term G2P- Amended Reactors	1 - 70	-0.61 ± 0.45	0	0	0	0
	71 - 80		0.52 ± 0.46	0	0	0
	81 - 90	-1.56 ± 0.78	0.09 ± 0.08	0.25 ± 0.22	-2.97 ± 1.28	0
	90-100		-0.23 ± 0.25			0
	101 - 130	-1.73 ± 0.74	0	0.84 ± 0.25	-1.22 ± 0.98	-20.1 ± 7.3
	130-187		0	0.89 ± 0.47		
	188-200	0	0	0	0	-12.5 ± 7.83

#### **4.4 Evidence for Biomineralization of Uranium Phosphate Minerals**

Chemical processes also contribute to uranium removal from groundwater. To demonstrate that the biomineralization of uranium phosphate minerals is a mechanism of uranium removal under anaerobic conditions, adsorption of uranium and possible uranium reduction processes must be quantified.

The results of the adsorption study on the soils used in this experiment indicate that uranium adsorption is favorable between pH 4.5 and 10 (Figure 11) as already demonstrated with soils from the ORFRC (Barnett et al. 2002). These findings suggest that at the pH of the FTR incubations (pH 5.5), adsorption should be favorable and only dependent on the availability of soil surface sites. Adsorption could have been occurring after G2P was removed from both the long and short-term G2P amended reactors. Uranium was still removed from the influent at a rate of  $12.5 \pm 7.83 \mu\text{M d}^{-1}$  for 12 days between days 188-200 in the long-term G2P amended reactors and  $10 \mu\text{M d}^{-1}$  for 99 days between days 101-200 in the short-term G2P-amended reactor (Table 3). Several lines of evidence indicate that U(VI) phosphate precipitation was the main removal process during the incubations in the presence of G2P and U(VI). First, rates of U(VI) removal were much higher in the presence of G2P in the long-term G2P incubations ( $20.1 \pm 7.3 \mu\text{M d}^{-1}$ ) compared to the short-term G2P incubation ( $10 \mu\text{M d}^{-1}$ ). Additionally, results from the solid phase extraction at the end of the incubation indicate that the majority of the uranium was in the form of uranyl phosphate precipitates (Figure 13) in both the short and long-term G2P amended reactors. The initial G2P input to the short-term G2P-amended reactor produced enough phosphate to precipitate some uranium as stable uranium phosphate mineral. However, the short-term G2P-amended reactor displayed

higher fractions of uranium as adsorbed or incorporated in iron or manganese oxides compared to the long-term G2P amended reactors, suggesting that uranium removal in this reactor was driven by adsorption processes. The anaerobic conditions and temporary rise in pH to ca. 8 could have made conditions favorable for respiration by uranium reduction. Uranium reduction (either direct or indirectly by ferrous iron) occurs at circumneutral pH in the absence of more favorable terminal electron acceptor (Lovley et al. 1991; Fredrickson et al. 2000). In these incubations, however, significant release of soluble uranium after re-introduction of oxygen to the system did not occur. Aerobic conditions were maintained for 80 days at the end of the incubations, and uranium levels remained less than 10  $\mu\text{M}$  in the effluent (Figure 11). Simultaneously, uranium speciation in the solid phase revealed uranium associated with phosphate minerals represents the major fraction of solid uranium at the end of the experiments (Figure 13). Other factors made the environment within the reactors inhospitable for the reduced uranium reduction and uraninite formation. Nitrate is a thermodynamically more favorable terminal electron acceptor than iron and uranium (Morel et al. 1993) and was constantly resupplied to the reactors. Additionally, nitrate (as well as nitrite) has been shown to reoxidize U(IV) (Wu et al. 2010).

#### **4.5 Implications and Further Research**

The results of this study indicate that the biomineralization of uranium phosphate minerals through the activity of acid phosphatases from the natural microbial community may occur in anaerobic environments exposed to exogenous addition of G2P. This process was demonstrated to occur both aerobically (Beazley et al., 2011) and anaerobically (this study) in similar flow through reactor incubations of ORFRC soils at pH 5.5. Uranium was removed from the influent solution under a range of pH conditions, though the increase in pH from 5.5 to 8 during G2P amendments caused a slight increase in dissolved uranium in the effluent of the long-term G2P amended reactors. This increase could have been caused by the production of bicarbonates due to the stimulation of microbial activity that could have solubilized uranium phosphates (Salome et al., 2012). Nevertheless, dissolved uranium levels at the output of the reactors remained much lower than the 200  $\mu\text{M}$  input continuously supplied to the reactors, suggesting that the immobilization of uranium was significant in these incubations. Uraninite produced by uranium reduction is an unlikely candidate due to the high instability of the uranium mineral under oxic conditions and in the presence of nitrite, a known oxidant of uraninite (Senko et al. 2002; Wan et al. 2005). The bulk chemical extractions of the soils performed as a function of distance from the inlet of the reactors indicate that the solid phase uranium formed in this study is primarily a uranyl phosphate precipitate. Further studies should be conducted to identify the composition of the uranium phosphate mineral, using a combination of synchrotron X-ray Absorption (XAS) and diffraction (XRD) spectroscopy, and investigate its long-term stability, especially in the presence of carbonate. The role nitrilotriacetic acid as a complexing agent of uranium (or other

organic ligands) should continue to be studied in order to further enhance the recovery of adsorbed uranium.

This and other studies show that biomineralization of uranium phosphate minerals can occur in both aerobic and anaerobic environments (Shelobolina et al. 2009; Beazley et al. 2011; Sivaswamy et al. 2011). As phosphatase activity is efficient at acidic pH (Rossolini et al. 1998), this strategy could be employed at sites where groundwater pH is too low for uranium reduction to be efficient or where alternative terminal electron acceptors (i.e. dissolved oxygen, nitrates) are available. Additionally, organophosphate sources disperse over larger distances than inorganic phosphate (Wellman et al. 2006) before reacting with the microbial community. Thus, the benefits of the non-reductive precipitation of uranium phosphate minerals make it an appealing remediation strategy that could be used in a wide range of environments. As G2P is an expensive organophosphate source, however, large-scale use of this substrate in remediation may be cost prohibitive, and the use of naturally-occurring organophosphate compounds should be investigated as alternative *in situ* bioremediation strategy.



## **CHAPTER 5**

### **CONCLUSIONS**

The objectives of this study were to (1) determine if the biomineralization of uranium phosphate minerals could occur under anaerobic conditions in a heterogeneous soil mixture, (2) identify the anaerobic respiration process that promoted the biomineralization uranium, (3) modify a sequential extraction procedure to distinguish between loosely adsorbed uranium and uranium phosphate precipitates, and (4) evaluate the solid phase speciation of uranium precipitated in anaerobic conditions during exogenous organophosphate amendments in flow-through reactors. The results of this study indicate that G2P is hydrolyzed by nitrate-reducing bacteria in anaerobic soils from the OFRC at low to neutral pH through a process that may couple both carbon and phosphorus metabolism. Uranium is removed in the long-term G2P amended reactors as well as the short-term G2P reactors, indicating that multiple immobilization processes play a role in uranium removal. A new extraction scheme modified from the method of Tessier that was optimized to differentiate adsorbed uranium from uranium phosphate precipitates indicated that both short and long-term G2P amended reactors removed aqueous uranium through microbially-mediated precipitation of uranium phosphate minerals, though the short-term G2P additions also resulted in significant adsorption of uranium onto iron or manganese oxides.

Overall, these incubations reveal that the biomineralization of uranium phosphate is a viable remediation strategy under both anaerobic and aerobic conditions in low to neutral pH and high nitrate environments. As phosphatase activity is efficient at acidic pH, this strategy could be employed at sites where groundwater pH is too low for

uranium reduction to be efficient. As organophosphate may disperse over large distances, this remediation strategy could be used in large contaminated areas, though the cost of exogenous organophosphate addition may warrant the investigation of naturally-occurring organophosphate compounds as alternative bioremediation strategy.

# APPENDIX A

## RATE CALCULATIONS FITTED TO DATA

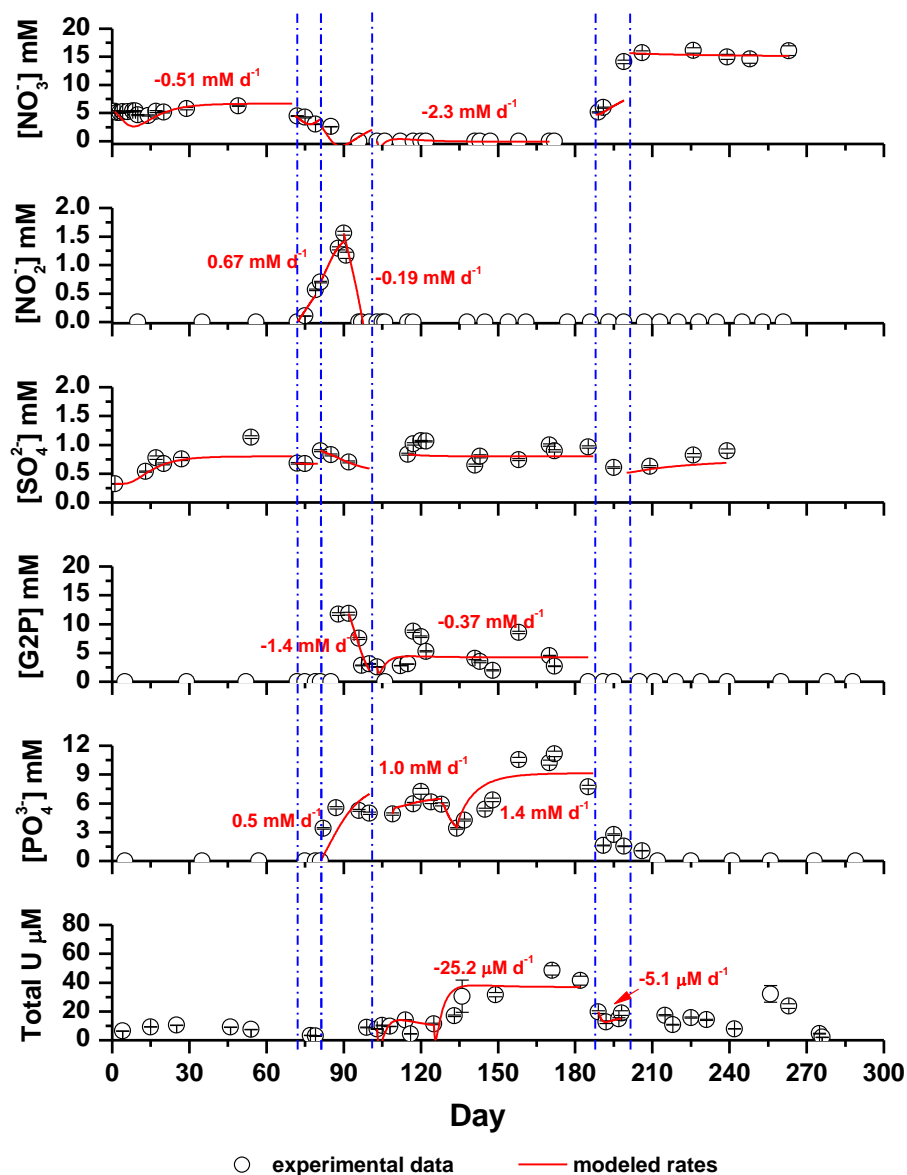


Figure A 1. Measurements (symbols) and calculated rates (line) of effluent concentrations of  $\text{NO}_3^-$ ,  $\text{NO}_2^-$ ,  $\text{SO}_4^{2-}$ , G2P,  $\text{PO}_4^{3-}$ , and total uranium over flow through reactor incubation from reactor 1. Vertical dashed lines at days 71, 81, 101, 188, and 200 correspond to removal of oxygen, introduction of 20 mM G2P, introduction of uranium, removal of G2P, and removal of uranium (repectively) to/from the input solution. Non-zero calculated rates are indicated on the figure.

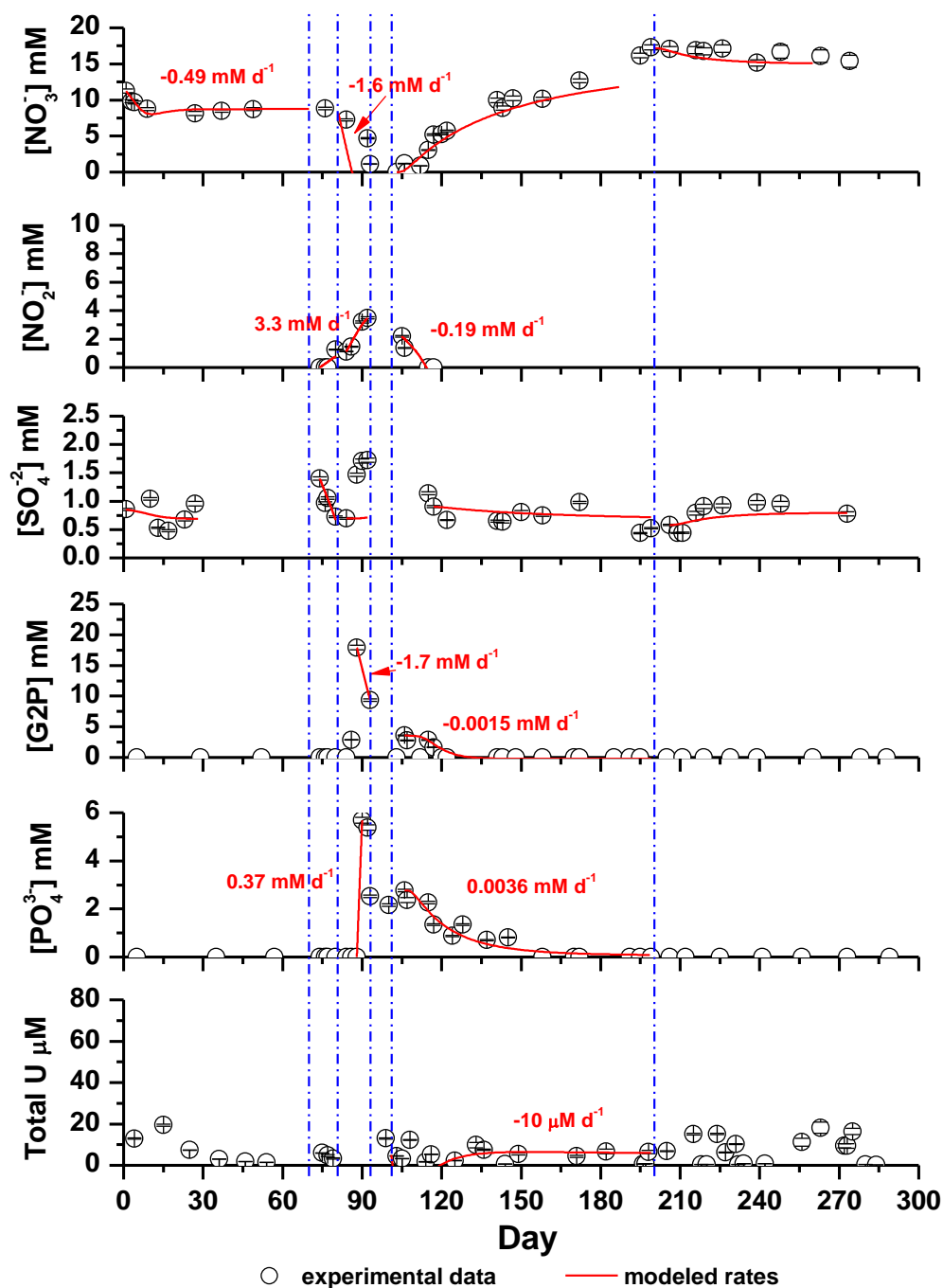


Figure A 2. Measurements (symbols) and calculated rates (line) of effluent concentrations of  $\text{NO}_3^-$ ,  $\text{NO}_2^-$ ,  $\text{SO}_4^{2-}$ , G2P,  $\text{PO}_4^{3-}$ , and total uranium over flow through reactor incubation from reactor 1. Vertical dashed lines at days 71, 81, 93, 101 and 200 correspond to removal of oxygen, introduction of 20 mM G2P, removal of G2P, introduction of uranium, and removal of uranium (repectively) to/from the input solution. Non-zero calculated rates are indicated on the figure.

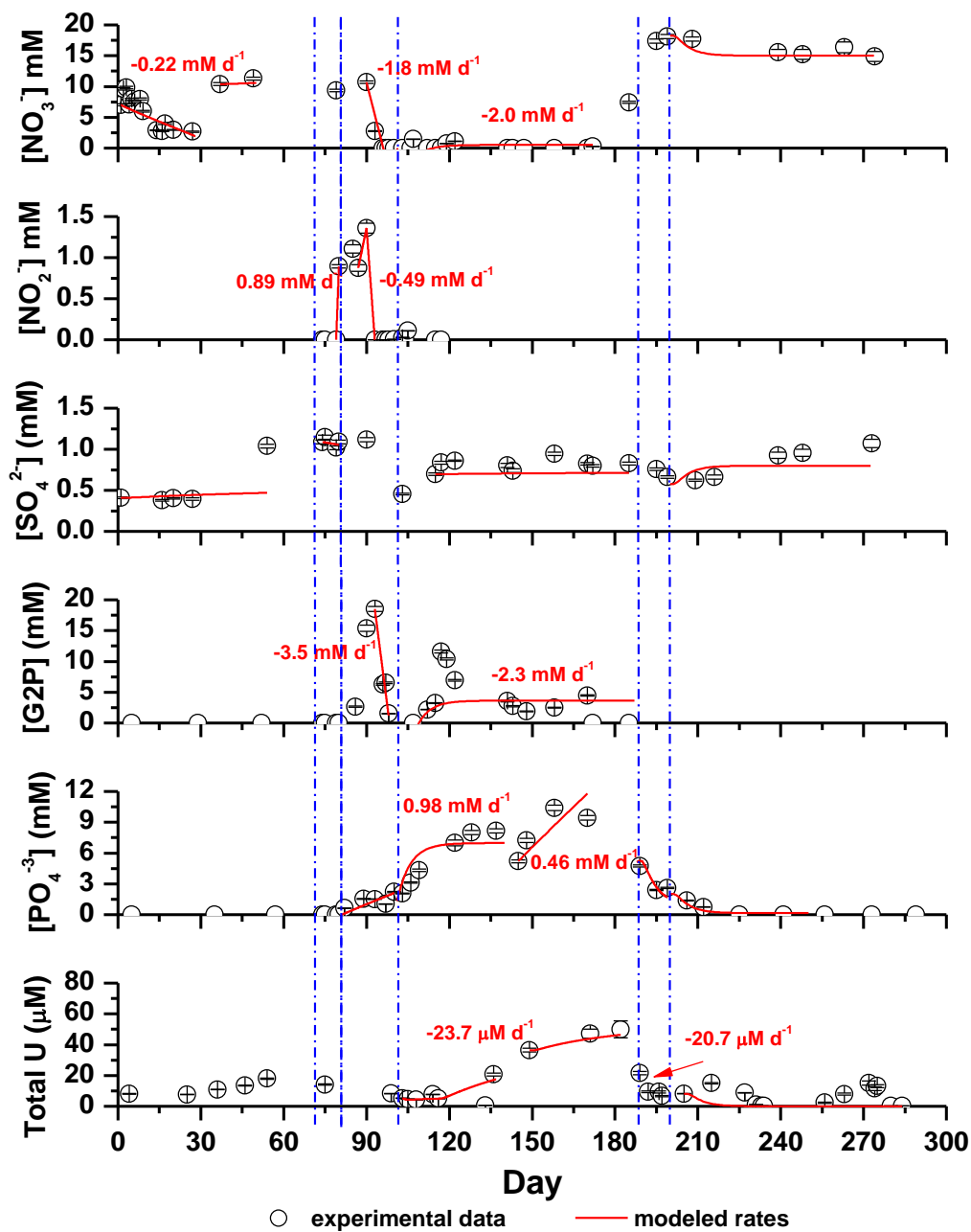


Figure A 3. Measurements (symbols) and calculated rates (line) of effluent concentrations of  $\text{NO}_3^-$ ,  $\text{NO}_2^-$ ,  $\text{SO}_4^{2-}$ , G2P,  $\text{PO}_4^{3-}$ , and total uranium over flow through reactor incubation from reactor 1. Vertical dashed lines at days 71, 81, 101, 188, and 200 correspond to removal of oxygen, introduction of 20 mM G2P, introduction of uranium, removal of G2P, and removal of uranium (repectively) to/from the input solution. Non-zero calculated rates are indicated on the figure.

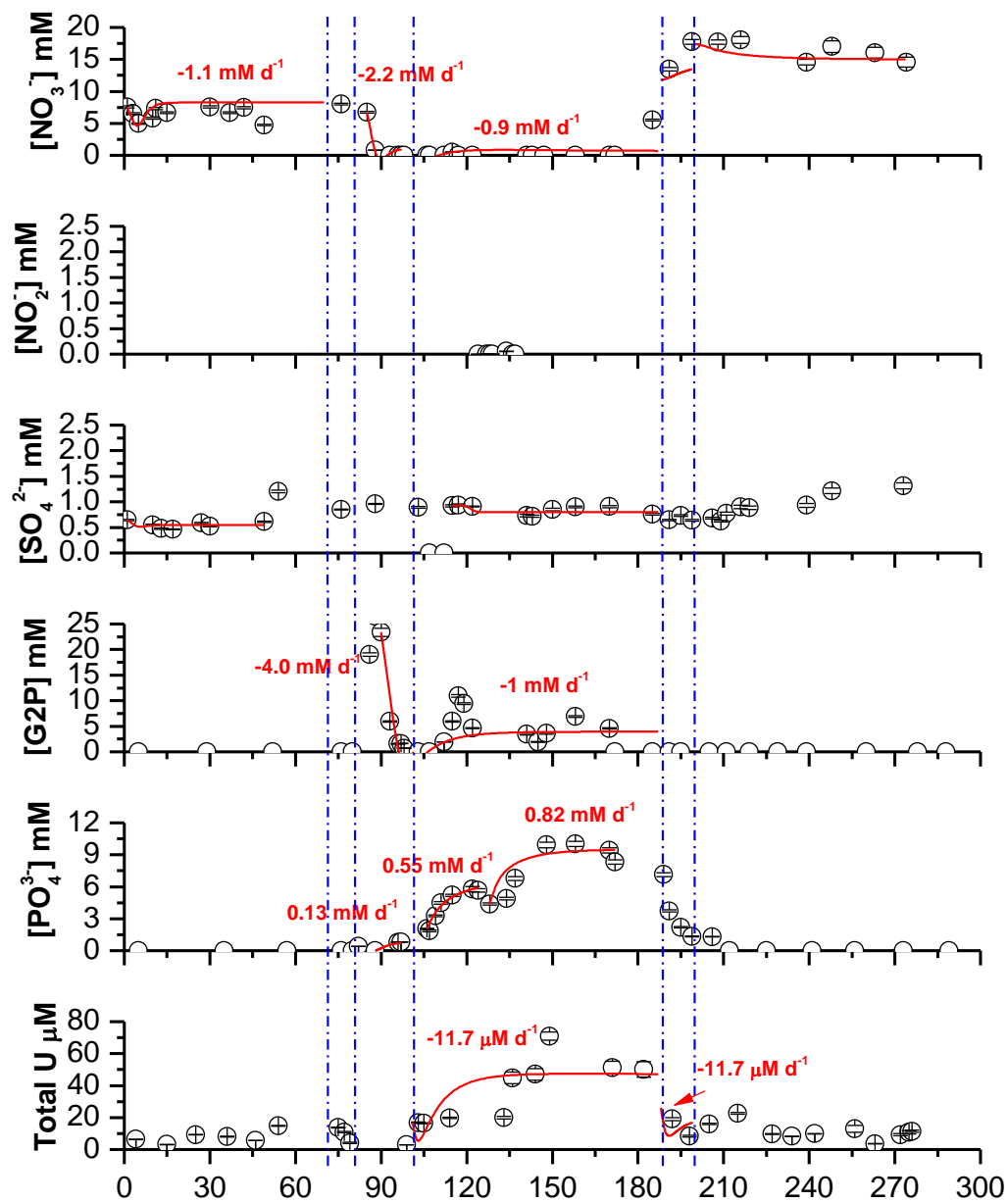


Figure A 4. Measurements (symbols) and calculated rates (line) of effluent concentrations of  $\text{NO}_3^-$ ,  $\text{NO}_2^-$ ,  $\text{SO}_4^{2-}$ , G2P,  $\text{PO}_4^{3-}$ , and total uranium over flow through reactor incubation from reactor 1. Vertical dashed lines at days 71, 81, 101, 188, and 200 correspond to removal of oxygen, introduction of 20 mM G2P, introduction of uranium, removal of G2P, and removal of uranium (repectively) to/from the input solution. Non-zero calculated rates are indicated on the figure.

## REFERENCES

- Akob, D. M., H. J. Mills, et al. (2007). "Metabolically active microbial communities in uranium-contaminated subsurface sediments." Fems Microbiology Ecology **59**(1): 95-107.
- Allen, P. G., D. K. Shuh, et al. (1996). "EXAFS determinations of uranium structures: The uranyl ion complexed with tartaric, citric, and malic acids." Inorganic Chemistry **35**(3): 784-&.
- Barnett, M. O., P. M. Jardine, et al. (2002). "U(VI) adsorption to heterogeneous subsurface media: Application of a surface complexation model." Environmental Science & Technology **36**(5): 937-942.
- Beazley, M. J. (2009). "Nonreductive biomineralization of Uranium(VI) as a result of microbial phosphatase activity." Earth and Atmospheric Sciences. Atlanta, Georgia Institute of Technology. **Doctor of Philosophy**: 225.
- Beazley, M. J., R. J. Martinez, et al. (2007). "Uranium biomineralization as a result of bacterial phosphatase activity: Insights from bacterial isolates from a contaminated subsurface." Environmental Science & Technology **41**(16): 5701-5707.
- Beazley, M. J., R. J. Martinez, et al. (2009). "Nonreductive Biomineralization of Uranium(VI) Phosphate Via Microbial Phosphatase Activity in Anaerobic Conditions." Geomicrobiology Journal **26**(7): 431-441.
- Beazley, M. J., R. J. Martinez, et al. (2011). "The effect of pH and natural microbial phosphatase activity on the speciation of uranium in subsurface soils." Geochimica Et Cosmochimica Acta **75**(19): 5648-5663.
- Behrends, T. and P. Van Cappellen (2005). "Competition between enzymatic and abiotic reduction of uranium(VI) under iron reducing conditions." Chemical Geology **220**(3-4): 315-327.
- Bernier-Latmani, R., H. Veeramani, et al. (2010). "Non-uraninite Products of Microbial U(VI) Reduction." Environmental Science & Technology **44**(24): 9456-9462.
- Blanco, P., F. V. Tome, et al. (2004). "Sequential extraction for radionuclide fractionation in soil samples: a comparative study." Applied Radiation and Isotopes **61**(2-3): 345-350.
- Boland, D. D., R. N. Collins, et al. (2011). "Effect of Amorphous Fe(III) Oxide Transformation on the Fe(II)-Mediated Reduction of U(VI)." Environmental Science & Technology **45**(4): 1327-1333.

- Boyanov, M. I., K. E. Fletcher, et al. (2011). "Solution and Microbial Controls on the Formation of Reduced U(IV) Species." Environmental Science & Technology **45**(19): 8336-8344.
- Brooks, S. C. (2001). Waste Characteristics of the Former S-3 Ponds and Outline of Uranium Chemistry Relevant to NABIR Field Research Center Studies.
- Butler, A. J., D. S. Hallett, et al. (1991). "Phosphatase production by a *Citrobacter* sp growing in batch culture and use of batch cultures to investigate some limitations in the use of polyacrylamide gel-immobilized cells for product release." Enzyme and Microbial Technology **13**(9): 716-721.
- Carey, E. and M. Taillefert (2005). "The role of soluble Fe(III) in the cycling of iron and sulfur in coastal marine sediments." Limnology and Oceanography **50**(4): 1129-1141.
- Cheng, T., M. O. Barnett, et al. (2004). "Effects of phosphate on uranium(VI) adsorption to goethite-coated sand." Environmental Science & Technology **38**(22): 6059-6065.
- DOE (1997). Linking Legacies - Connecting the cold war nuclear weapons production processes to their environmental consequences. Washington D.C., Office of Environmental Management - The U.S. Department of Energy.
- Fletcher, K. E., M. I. Boyanov, et al. (2010). "U(VI) Reduction to Mononuclear U(IV) by *Desulfitobacterium* Species." Environmental Science & Technology **44**(12): 4705-4709.
- Fomina, M., J. M. Charnock, et al. (2007). "Fungal transformations of uranium oxides." Environmental Microbiology **9**(7): 1696-1710.
- Fredrickson, J. K., J. M. Zachara, et al. (2000). "Reduction of U(VI) in goethite ( $\alpha$ -FeOOH) suspensions by a dissimilatory metal-reducing bacterium." Geochimica Et Cosmochimica Acta **64**(18): 3085-3098.
- Fuller, C. C., J. R. Bargar, et al. (2003). "Molecular-scale characterization of uranium sorption by bone apatite materials for a permeable reactive barrier demonstration." Environmental Science & Technology **37**(20): 4642-4649.
- Gavrilescu, M., L. V. Pavel, et al. (2009). "Characterization and remediation of soils contaminated with uranium." Journal of Hazardous Materials **163**(2-3): 475-510.
- Geissler, A., M. Merroun, et al. (2009). "Biogeochemical changes induced in uranium mining waste pile samples by uranyl nitrate treatments under anaerobic conditions." Geobiology **7**(3): 282-294.



- Gonzalez, P. J., C. Correia, et al. (2006). "Bacterial nitrate reductases: Molecular and biological aspects of nitrate reduction." Journal of Inorganic Biochemistry **100**(5-6): 1015-1023.
- Haas, J. R. and A. Northup (2004). "Effects of aqueous complexation on reductive precipitation of uranium by *Shewanella putrefaciens*." Geochemical Transactions **5**(3): 41-48.
- Jardine, P. M., Watson, D. B., Blake, D. A., Beard, L. P., Brooks, S. C., Carley, J. M., , C. S. Criddle, Doll, W. E., Fields, M. W., Fendorf, S. E., Geesey, G. G., Ginder-, et al. (2006). Techniques for assessing the performance of in situ bioreduction and immobilization of metals and radionuclides in contaminated subsurface environments.
- Jerden, J. L. and A. K. Sinha (2003). "Phosphate based immobilization of uranium in an oxidizing bedrock aquifer." Applied Geochemistry **18**(6): 823-843.
- Khijniak, T. V., A. I. Slobodkin, et al. (2005). "Reduction of uranium(VI) phosphate during growth of the thermophilic bacterium *Thermoterrabacterium ferrireducens*." Applied and Environmental Microbiology **71**(10): 6423-6426.
- Lam, P. and M. M. M. Kuypers (2011). Microbial Nitrogen Cycling Processes in Oxygen Minimum Zones. Annual Review of Marine Science, Vol 3. C. A. Carlson and S. J. Giovannoni. Palo Alto, Annual Reviews. **3**: 317-345.
- Langmuir (1997). Aqueous Environmental Geochemistry. 600.
- Lenhart, J. J. and B. D. Honeyman (1999). "Uranium(VI) sorption to hematite in the presence of humic acid." Geochimica Et Cosmochimica Acta **63**(19-20): 2891-2901.
- Liger, E., L. Charlet, et al. (1999). "Surface catalysis of uranium(VI) reduction by iron(II)." Geochimica Et Cosmochimica Acta **63**(19-20): 2939-2955.
- Lovley, D. R. and E. J. P. Phillips (1992). "Reduction of uranium by *Desulfovibrio desulfuricans*." Applied and Environmental Microbiology **58**(3): 850-856.
- Lovley, D. R., E. J. P. Phillips, et al. (1991). "Microbial reduction of uranium." Nature **350**(6317): 413-416.
- Macaskie, L. E., K. M. Bonthron, et al. (1994). "Phosphatase-mediated heavy-metal accumulation by a *Citrobacter* sp and related enterobacteria." Fems Microbiology Letters **121**(2): 141-146.

- Martinez, R. J., M. J. Beazley, et al. (2008). "Aerobic uranium(VI) bioprecipitation by metal-resistant bacteria isolated from radionuclide- and metal-contaminated subsurface soils (vol 9, pg 3122, 2008)." Environmental Microbiology **10**(4): 1097-1097.
- Michalsen, M. M., A. D. Peacock, et al. (2009). "Treatment of Nitric Acid-, U(VI)-, and Tc(VII)-Contaminated Groundwater in Intermediate-Scale Physical Models of an In Situ Biobarrier." Environmental Science & Technology **43**(6): 1952-1961.
- Morel, F. M. M. and J. G. Hering (1993). Principles and Applications of Aquatic Chemistry. New York, John Wiley & Sons, Inc.
- Murphy, J. and J. P. Riley (1962). "A modified single solution method for determination of phosphate in natural waters." Analytica Chimica Acta **26**(1): 31-&.
- Ohnuki, T., T. Ozaki, et al. (2005). "Mechanisms of uranium mineralization by the yeast *Saccharomyces cerevisiae*." Geochimica Et Cosmochimica Acta **69**(22): 5307-5316.
- Pallud, C., C. Meile, et al. (2007). "The use of flow-through sediment reactors in biogeochemical kinetics: Methodology and examples of applications." Marine Chemistry **106**(1-2): 256-271.
- Renninger, N., R. Knopp, et al. (2004). "Uranyl precipitation by *Pseudomonas aeruginosa* via controlled polyphosphate metabolism." Applied and Environmental Microbiology **70**(12): 7404-7412.
- Rossolini, G. M., S. Schippa, et al. (1998). "Bacterial nonspecific acid phosphohydrolases: physiology, evolution and use as tools in microbial biotechnology." Cellular and Molecular Life Sciences **54**(8): 833-850.
- Roychoudhury, A. N., E. Viollier, et al. (1998). "A plug flow-through reactor for studying biogeochemical reactions in undisturbed aquatic sediments." Applied Geochemistry **13**(2): 269-280.
- Roychoudhury, A. N., E. Viollier, et al. (1998). "A plug flow-through reactor for studying biogeochemical reactions in undisturbed aquatic sediments." Applied Geochemistry **13**: 269-280.
- Salome, K. R., M. J. Beazley, et al. (2011). "Potential for utilizing naturally occurring phytate in U(VI) bioremediation strategies." Abstracts of Papers of the American Chemical Society **242**.
- Sandino, A. and J. Bruno (1992). "The solubility of  $(\text{UO}_2)_3(\text{PO}_4)_2 \cdot 4\text{H}_2\text{O}(\text{s})$  and the formation of U(VI) phosphate complexes - their influence in uranium speciation in natural-waters." Geochimica Et Cosmochimica Acta **56**(12): 4135-4145.

- Sanford, R. A., Q. Wu, et al. (2007). "Hexavalent uranium supports growth of Anaeromyxobacter dehalogenans and Geobacter spp. with lower than predicted biomass yields." Environmental Microbiology **9**(11): 2885-2893.
- Schecher, W. D. and D. C. McAvoy (2001). MINEQL+ A Chemical Equilibrium Modeling System, Version 4.5 for Windows, User's Manual. . Hallowell, Maine, Environmental Research Software.
- Schultz, M. K., W. C. Burnett, et al. (1998). "Evaluation of a sequential extraction method for determining actinide fractionation in soils and sediments." Journal of Environmental Radioactivity **40**(2): 155-174.
- Schwertmann, U. and R. M. Cornell (2000). Iron Oxides in the Laboratory Preparation and Characterization, Second Addition, Wiley-VCH: 93-97.
- Senko, J. M., J. D. Istok, et al. (2002). "In-situ evidence for uranium immobilization and remobilization." Environmental Science & Technology **36**(7): 1491-1496.
- Shan, X. Q. and C. Bin (1993). "Evaluation of sequential extraction for speciation of trace-metals in model soil containing natural minerals and humic-acid." Analytical Chemistry **65**(6): 802-807.
- Shelobolina, E. S., H. Konishi, et al. (2009). "U(VI) Sequestration in Hydroxyapatite Produced by Microbial Glycerol 3-Phosphate Metabolism." Applied and Environmental Microbiology **75**(18): 5773-5778.
- Sivaswamy, V., M. I. Boyanov, et al. (2011). "Multiple Mechanisms of Uranium Immobilization by Cellulomonas sp Strain ES6." Biotechnology and Bioengineering **108**(2): 264-276.
- Smith, R. M., A. E. Martell, et al. (2003). NIST Standard Reference Database 46.
- Smith, S. C., M. Douglas, et al. (2009). "Uranium Extraction From Laboratory-Synthesized, Uranium-Doped Hydrous Ferric Oxides." Environmental Science & Technology **43**(7): 2341-2347.
- Spain, A. M. and L. R. Krumholz (2011). "Nitrate-Reducing Bacteria at the Nitrate and Radionuclide Contaminated Oak Ridge Integrated Field Research Challenge Site: A Review." Geomicrobiology Journal **28**(5-6): 418-429.
- Stary, J. and J. Prasilova (1961). "Extraction and ion exchange investigation of uranium(VI) chelates." Journal of Inorganic & Nuclear Chemistry **17**(3-4): 361-365.

- Stewart, B. D., M. A. Mayes, et al. (2010). "Impact of Uranyl-Calcium-Carbonato Complexes on Uranium(VI) Adsorption to Synthetic and Natural Sediments." Environmental Science & Technology **44**(3): 928-934.
- Suzuki, Y., K. Tanaka, et al. (2010). "Effects of Citrate, NTA, and EDTA on the Reduction of U(VI) by *Shewanella putrefaciens*." Geomicrobiology Journal **27**(3): 245-250.
- Tebo, B. M. and A. Y. Obraztsova (1998). "Sulfate-reducing bacterium grows with Cr(VI), U(VI), Mn(IV), and Fe(III) as electron acceptors." Fems Microbiology Letters **162**(1): 193-198.
- Teleb, S. M., E. M. Nour, et al. (2005). "Synthesis and characterization of some uranyl and zirconyl nitrilotriacetic acid (NTA) chelates." Journal of Coordination Chemistry **58**(15): 1261-1269.
- Tessier, A., P. G. C. Campbell, et al. (1979). "Sequential extraction procedure for the speciation of particulate trace-metals." Analytical Chemistry **51**(7): 844-851.
- Thomas, R. A. P. and L. E. Macaskie (1996). "Biodegradation of tributyl phosphate by naturally occurring microbial isolates and coupling to the removal of uranium from aqueous solution." Environmental Science & Technology **30**(7): 2371-2375.
- Van Genuchten, M. T. (1981). "Analytical solution for chemical transport with simultaneous adsorption, zero-order production and first order decay." Journal of Hydrology **43**: 213-233.
- Vitousek, P. M. and R. W. Howarth (1991). "Nitrogen limitation on land and in the sea - how it can occur." Biogeochemistry **13**(2): 87-115.
- Wade, R. and T. J. DiChristina (2000). "Isolation of U(VI) reduction-deficient mutants of *Shewanella putrefaciens*." Fems Microbiology Letters **184**(2): 143-148.
- Waite, T. D., J. A. Davis, et al. (1994). "Uranium(VI) adsorption to ferrihydrite - application of a surface complexation model." Geochimica Et Cosmochimica Acta **58**(24): 5465-5478.
- Waldron, P. J., L. Y. Wu, et al. (2009). "Functional Gene Array-Based Analysis of Microbial Community Structure in Groundwaters with a Gradient of Contaminant Levels." Environmental Science & Technology **43**(10): 3529-3534.
- Wan, J. M., T. K. Tokunaga, et al. (2005). "Reoxidation of bio-reduced uranium under reducing conditions." Environmental Science & Technology **39**(16): 6162-6169.

- Wellman, D. M., J. P. Icenhower, et al. (2006). "Comparative analysis of soluble phosphate amendments for the remediation of heavy metal contaminants: Effect on sediment hydraulic conductivity." Environmental Chemistry **3**(3): 219-224.
- Wersin, P., M. F. Hochella, et al. (1994). "Interaction between aqueous uranium(VI) and minerals - spectroscopic evidence for sorption and reduction." Geochimica Et Cosmochimica Acta **58**(13): 2829-2843.
- Wu, W. M., J. Carley, et al. (2006). "Pilot-scale in situ bioremediation of uranium in a highly contaminated aquifer. 1. Conditioning of a treatment zone." Environmental Science & Technology **40**(12): 3978-3985.
- Wu, W. M., J. Carley, et al. (2010). "Effects of Nitrate on the Stability of Uranium in a Bioreduced Region of the Subsurface." Environmental Science & Technology **44**(13): 5104-5111.
- Zhou, P. and B. H. Gu (2005). "Extraction of oxidized and reduced forms of uranium from contaminated soils: Effects of carbonate concentration and pH." Environmental Science & Technology **39**(12): 4435-4440.
- Zumft, W. G. (1997). "Cell biology and molecular basis of denitrification." Microbiology and Molecular Biology Reviews **61**(4): 533-+.